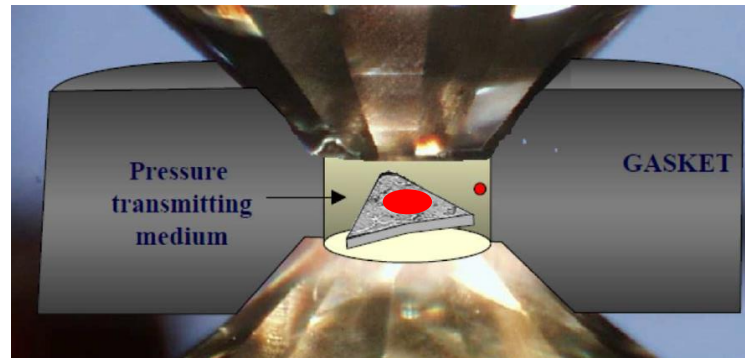


Phase transitions in laser heated diamond anvil cell: observations from in situ and ex situ analyses



Different type of phase transitions

- First order solid solid transition
- Second order solid solid transition
- Congruent melting
- Incongruent melting

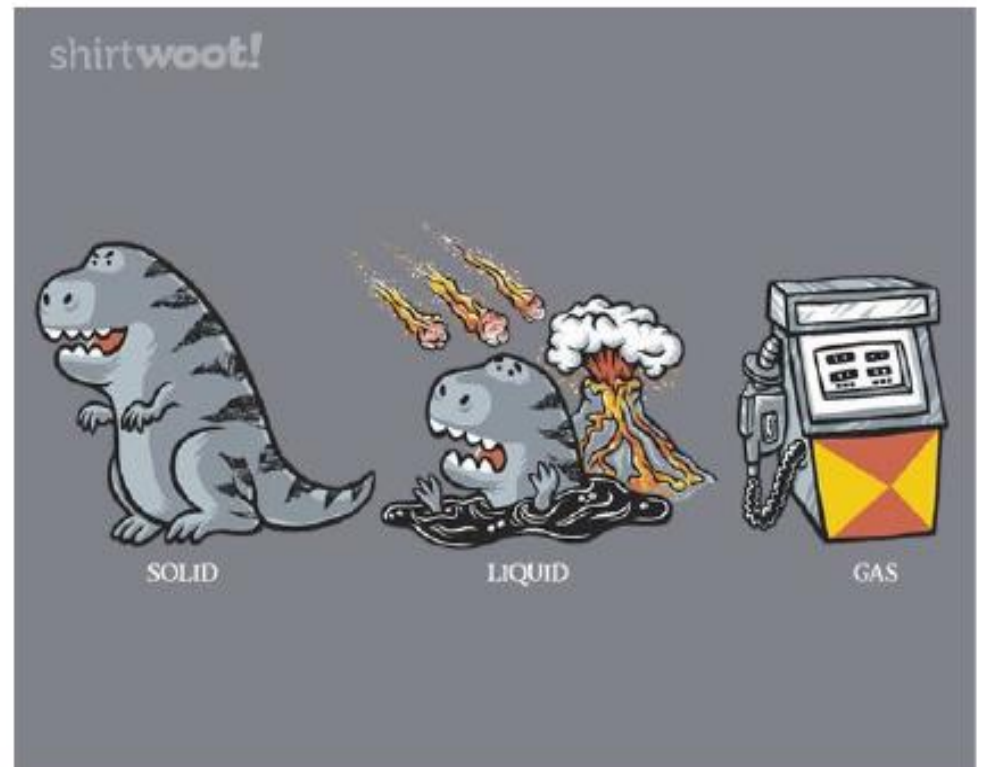
Different type of phase transitions

-First order solid solid transition

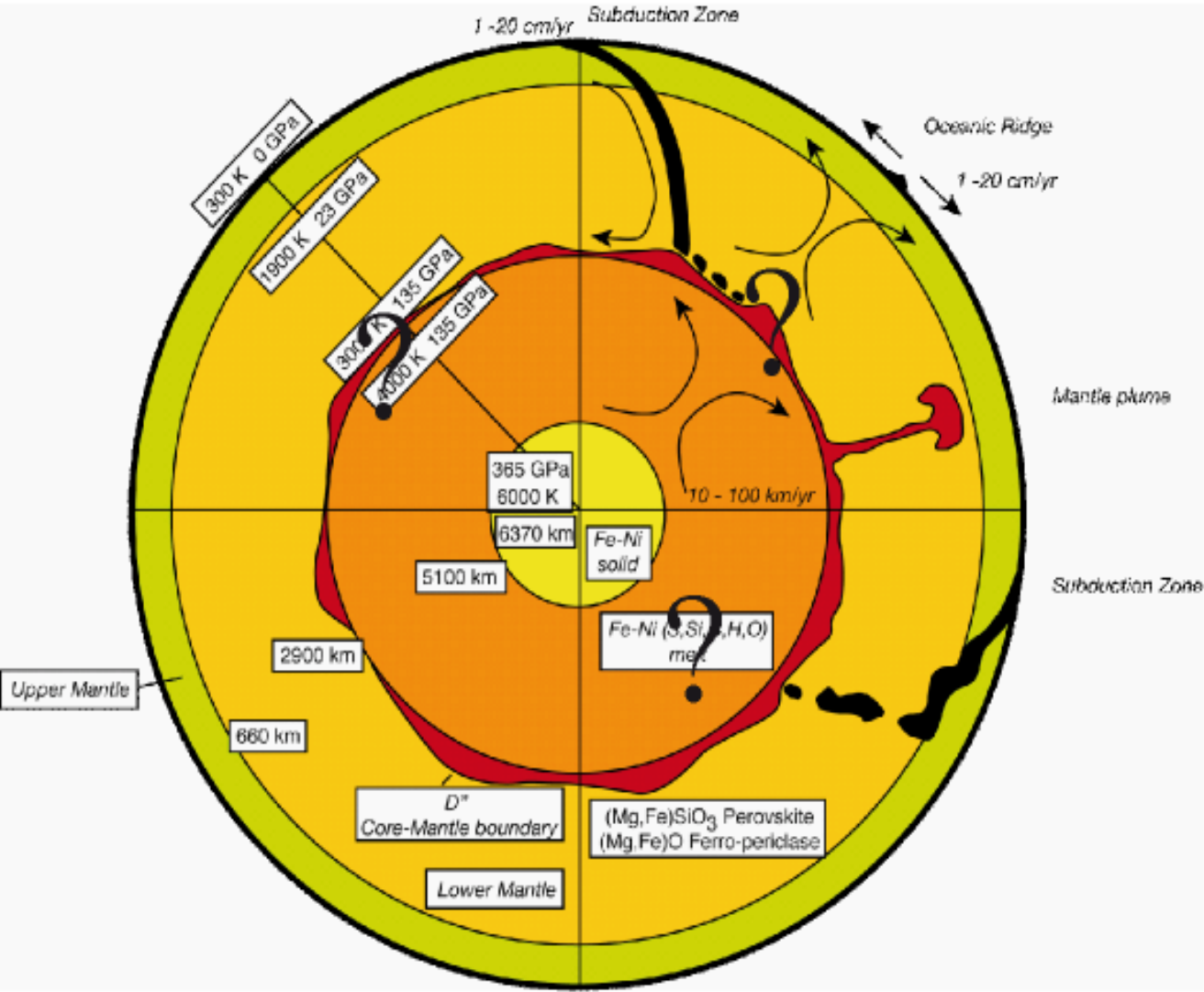
-Second order solid solid transition

-Congruent melting

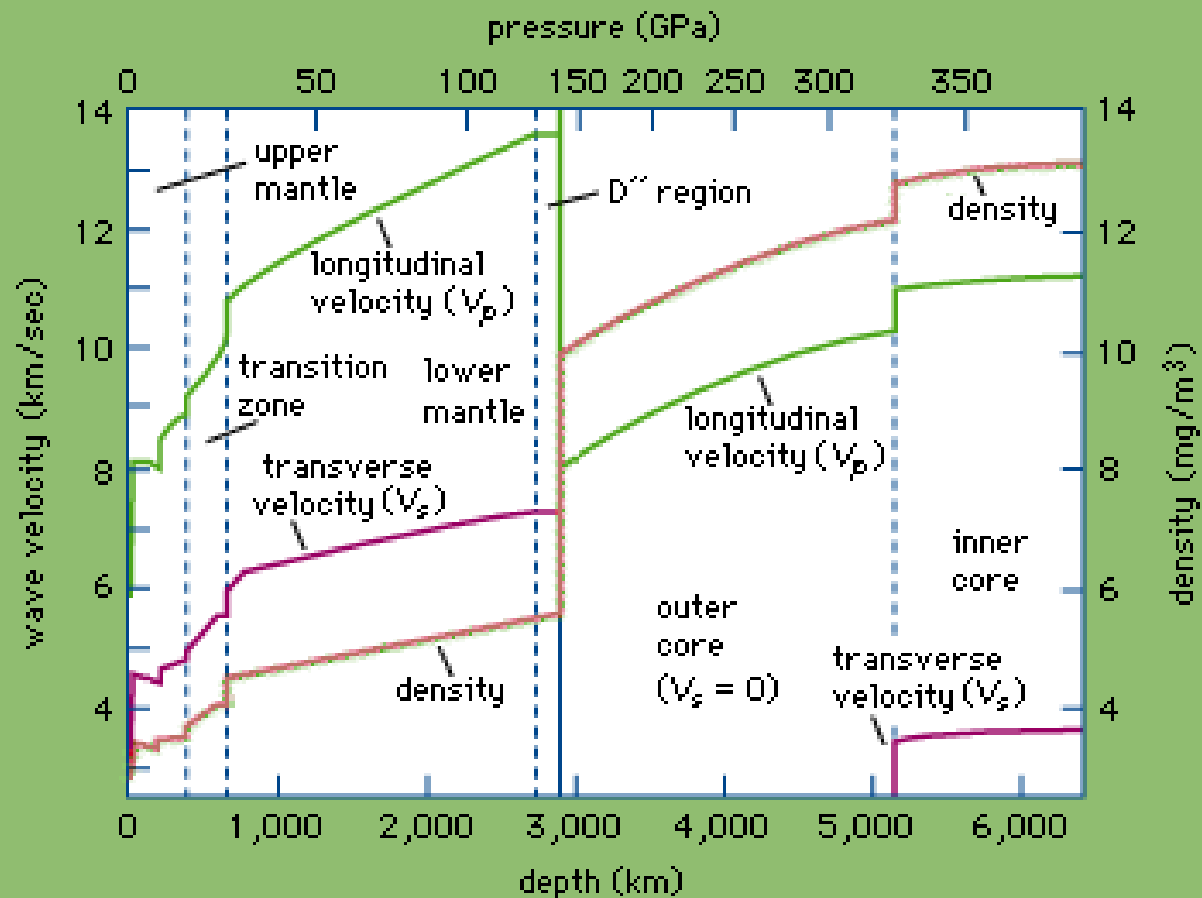
-Incongruent melting



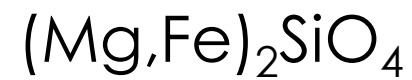
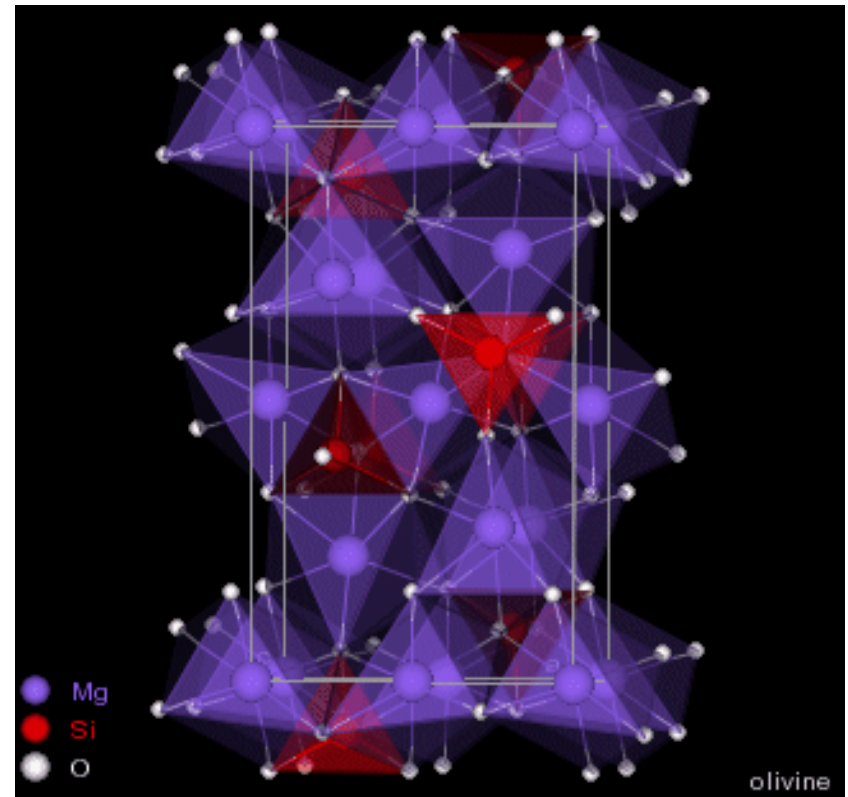
Internal structure of the Earth



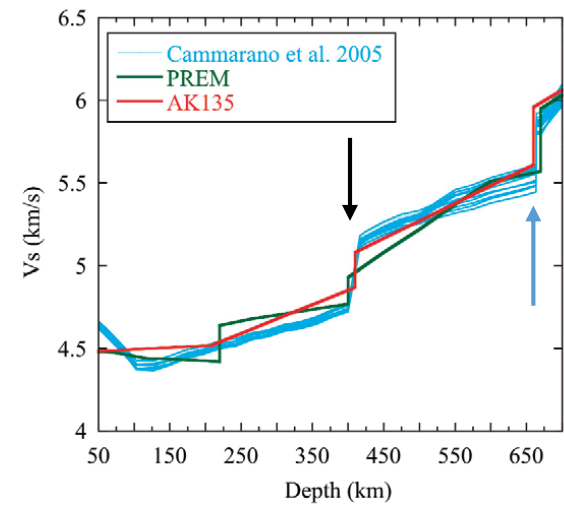
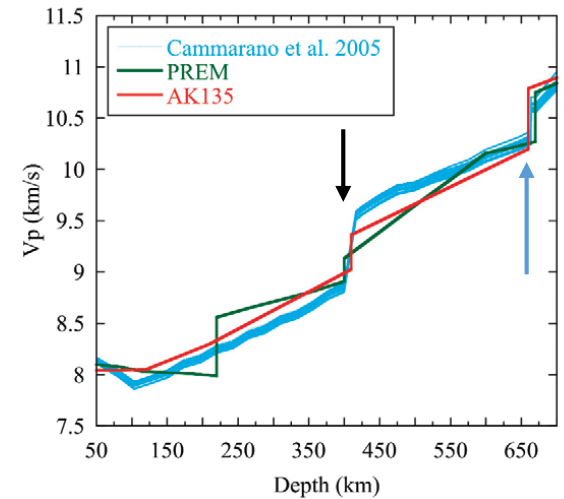
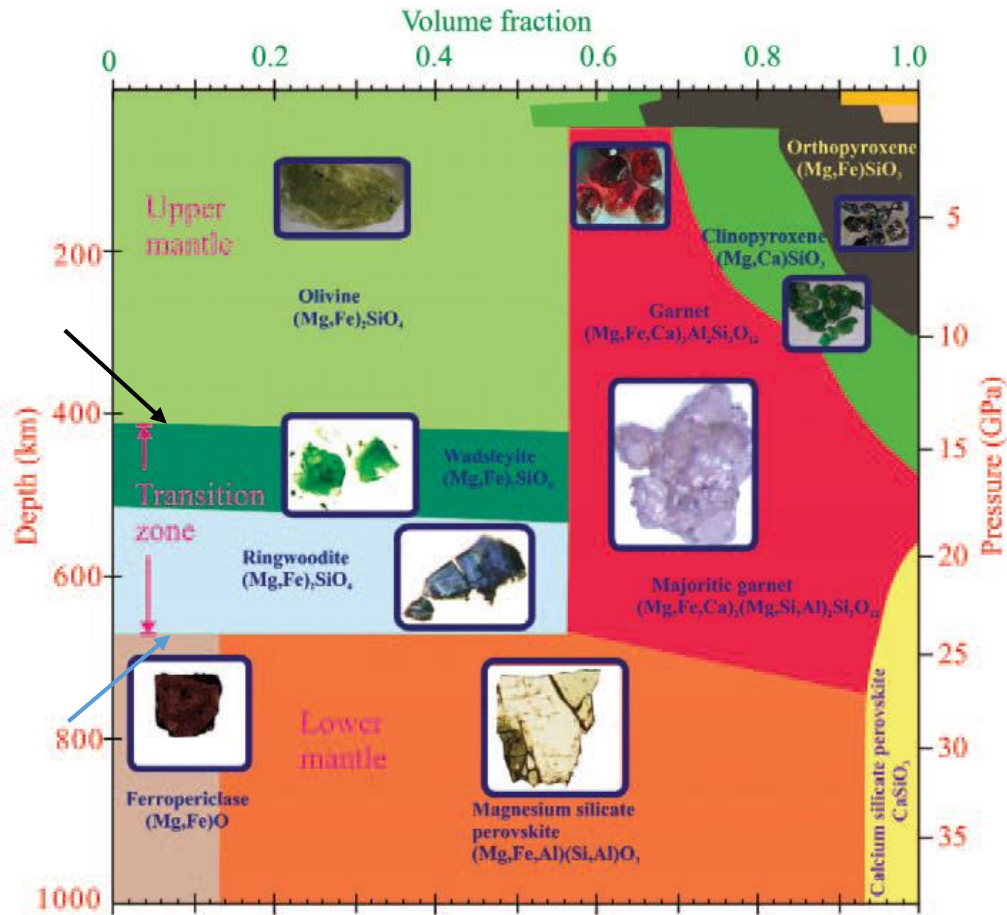
Information on the Earth's interior



Olivine: 60% en volume des roches du manteau supérieur

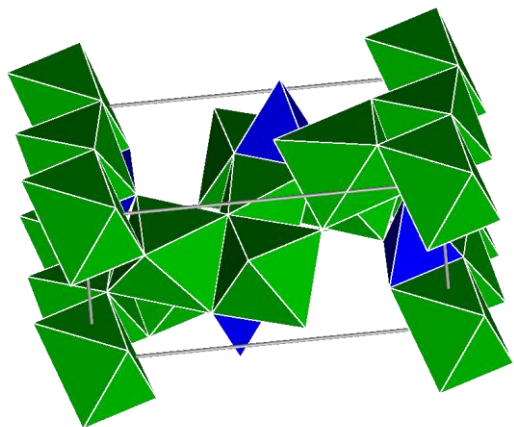


Strong relation between seismological structure of the upper mantle and its mineralogy

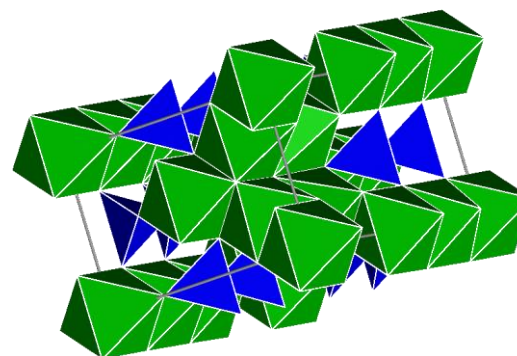


Transitions de phases induites par la pression

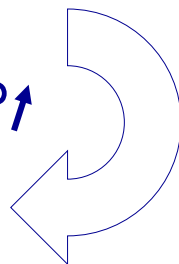
α -olivine $(\text{Mg,Fe})_2\text{SiO}_4$



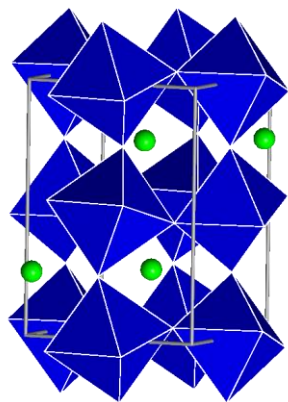
β -wadsleyite $(\text{Mg,Fe})_2\text{SiO}_4$



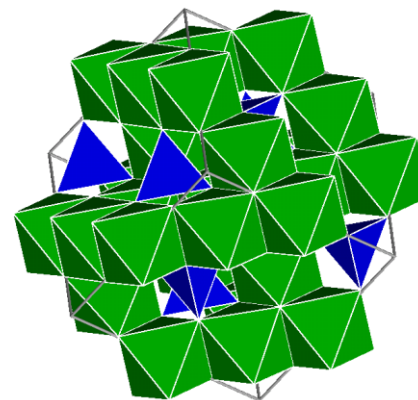
$P \uparrow$



Perovskite $(\text{Mg,Fe})\text{SiO}_3$



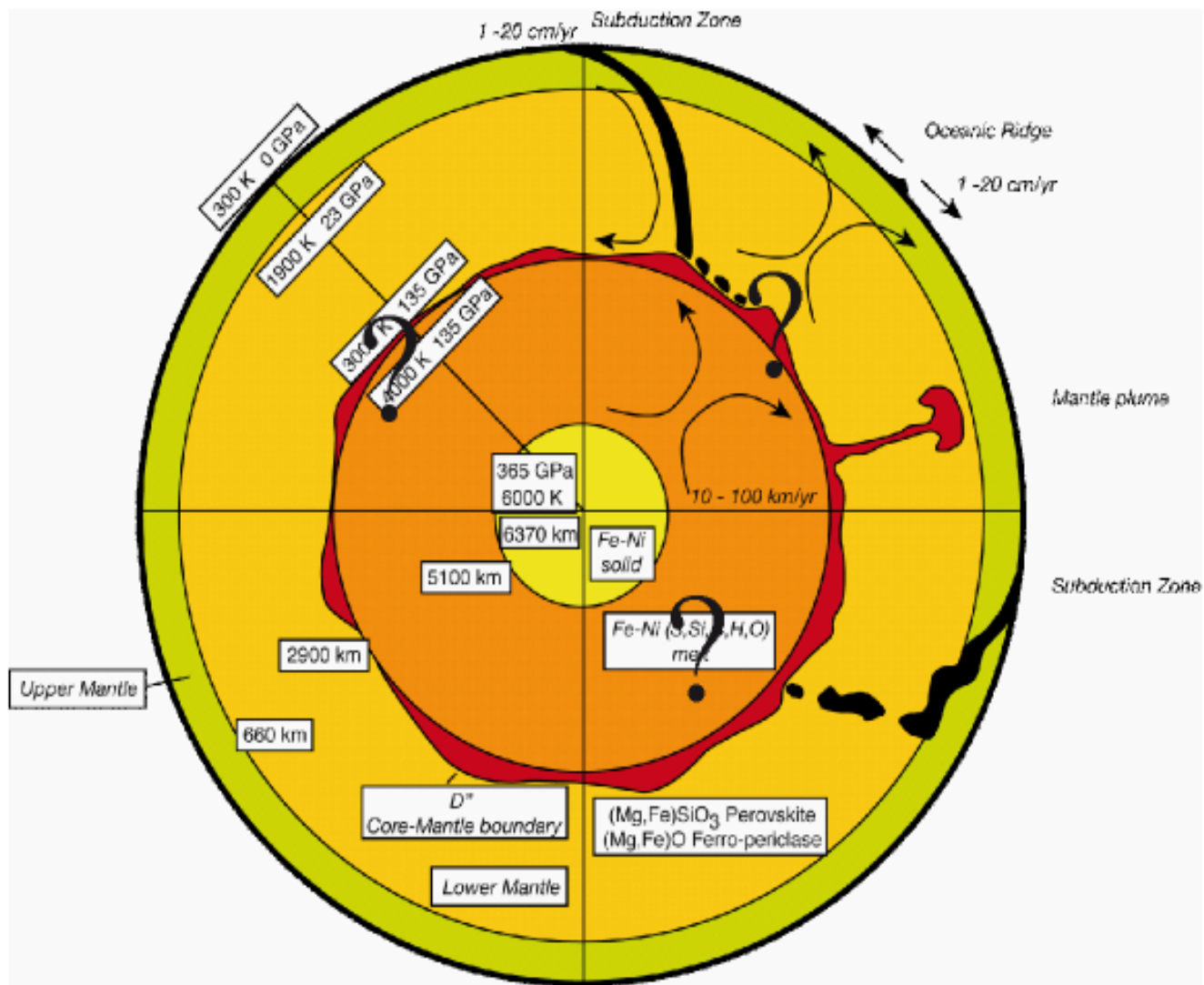
γ -ringwoodite $(\text{Mg,Fe})_2\text{SiO}_4$



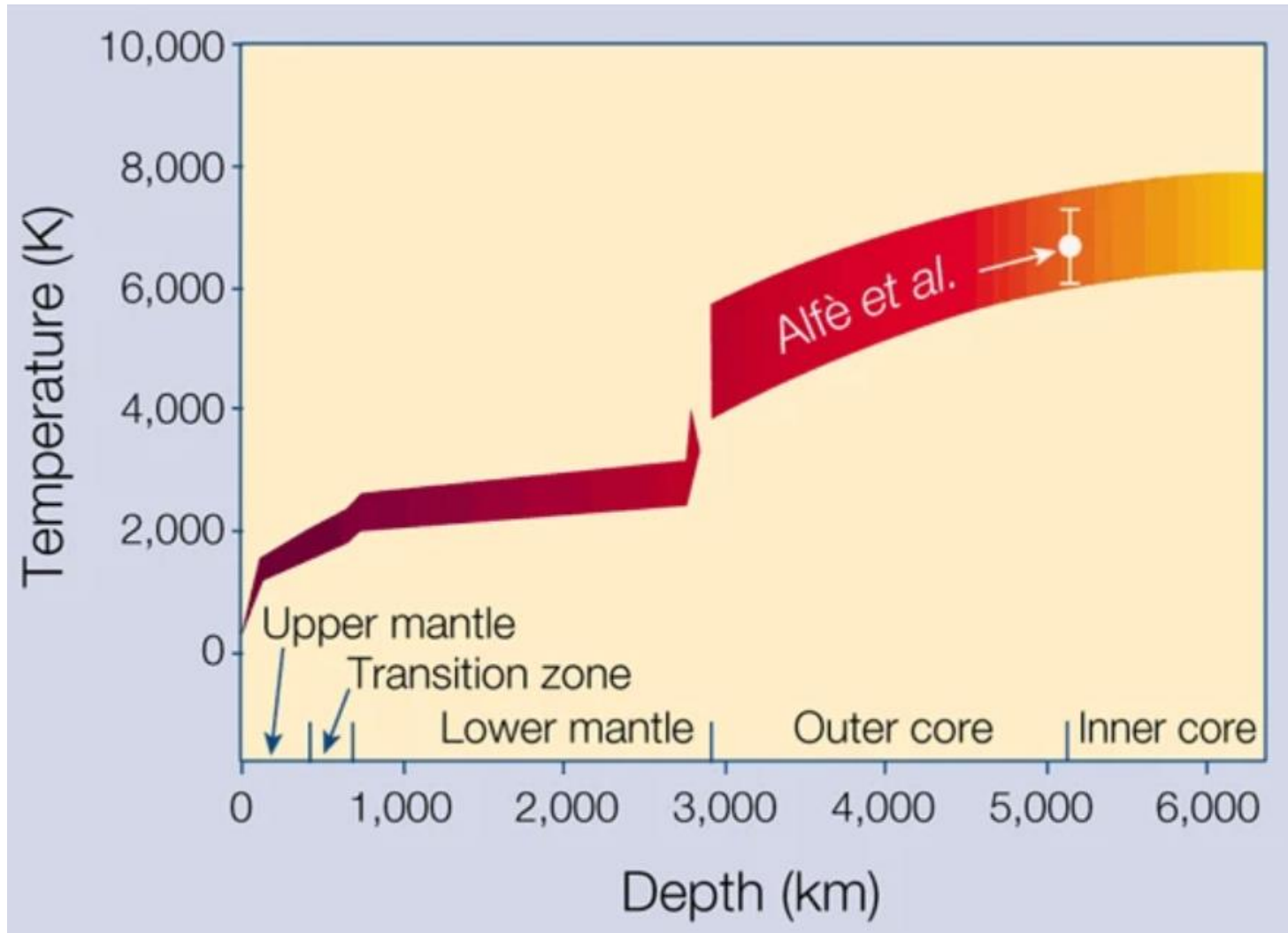
$+(\text{Mg,Fe})\text{O}$

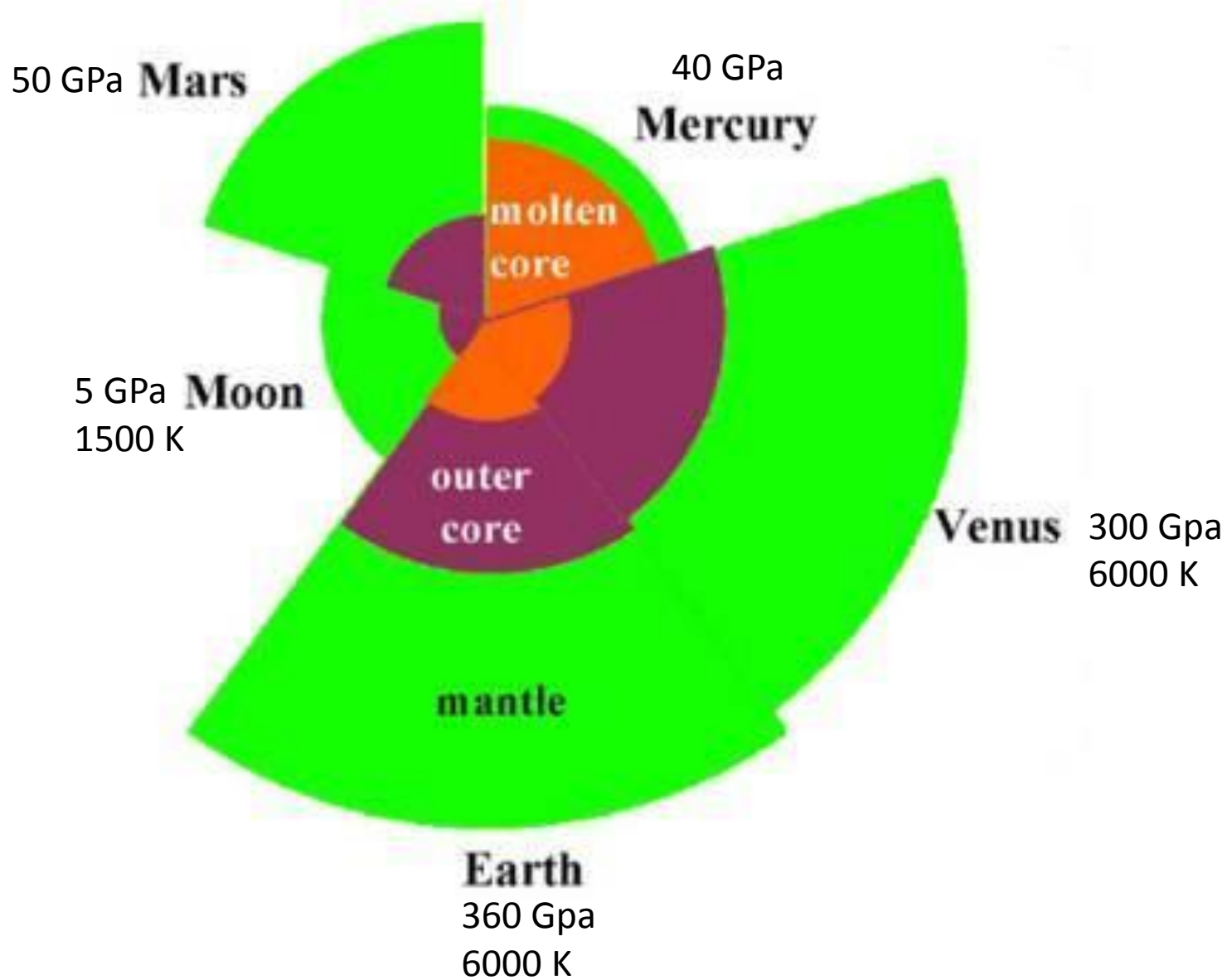


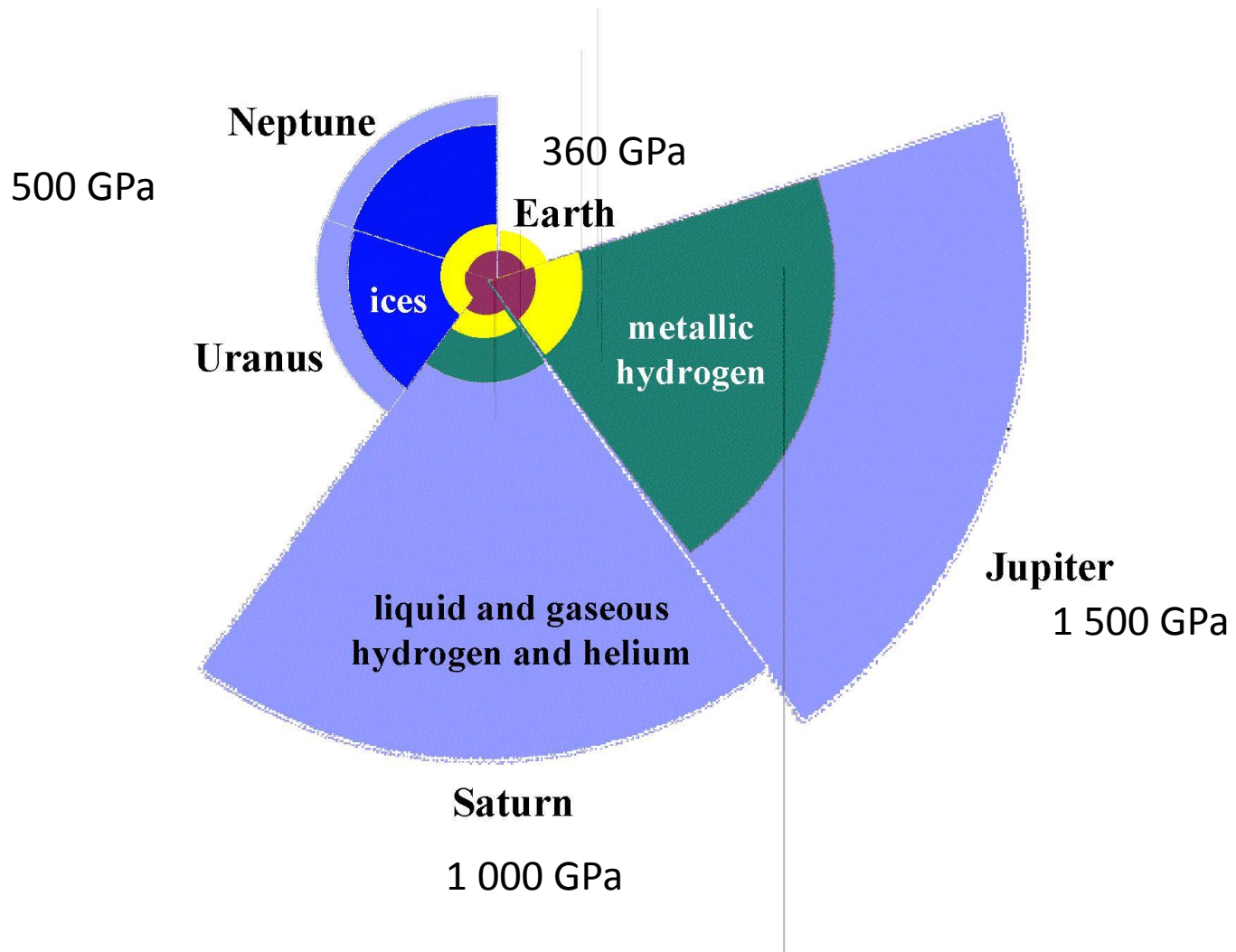
Internal structure of the Earth



Melting of core materials at ICB : anchoring point for the geotherm



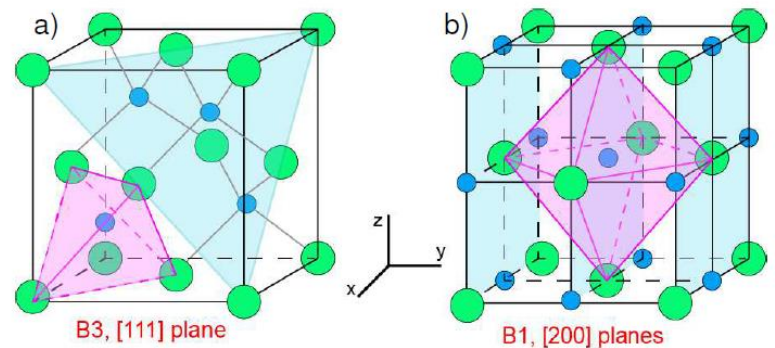
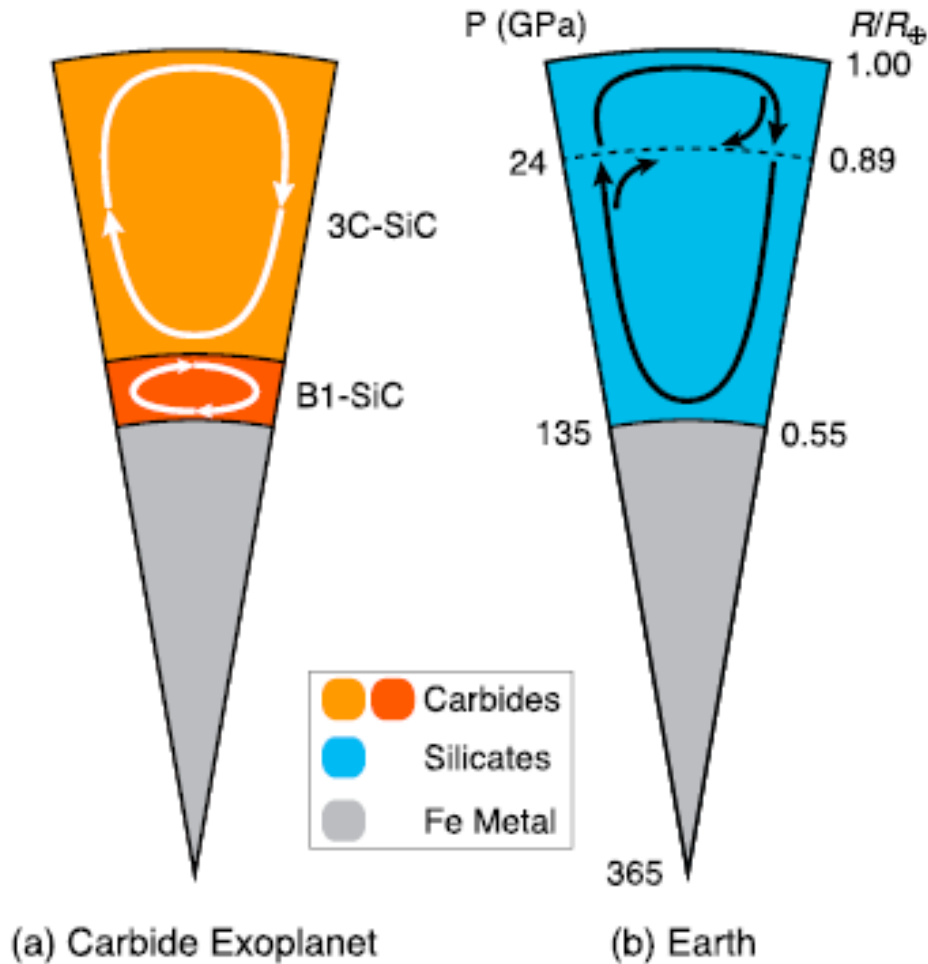




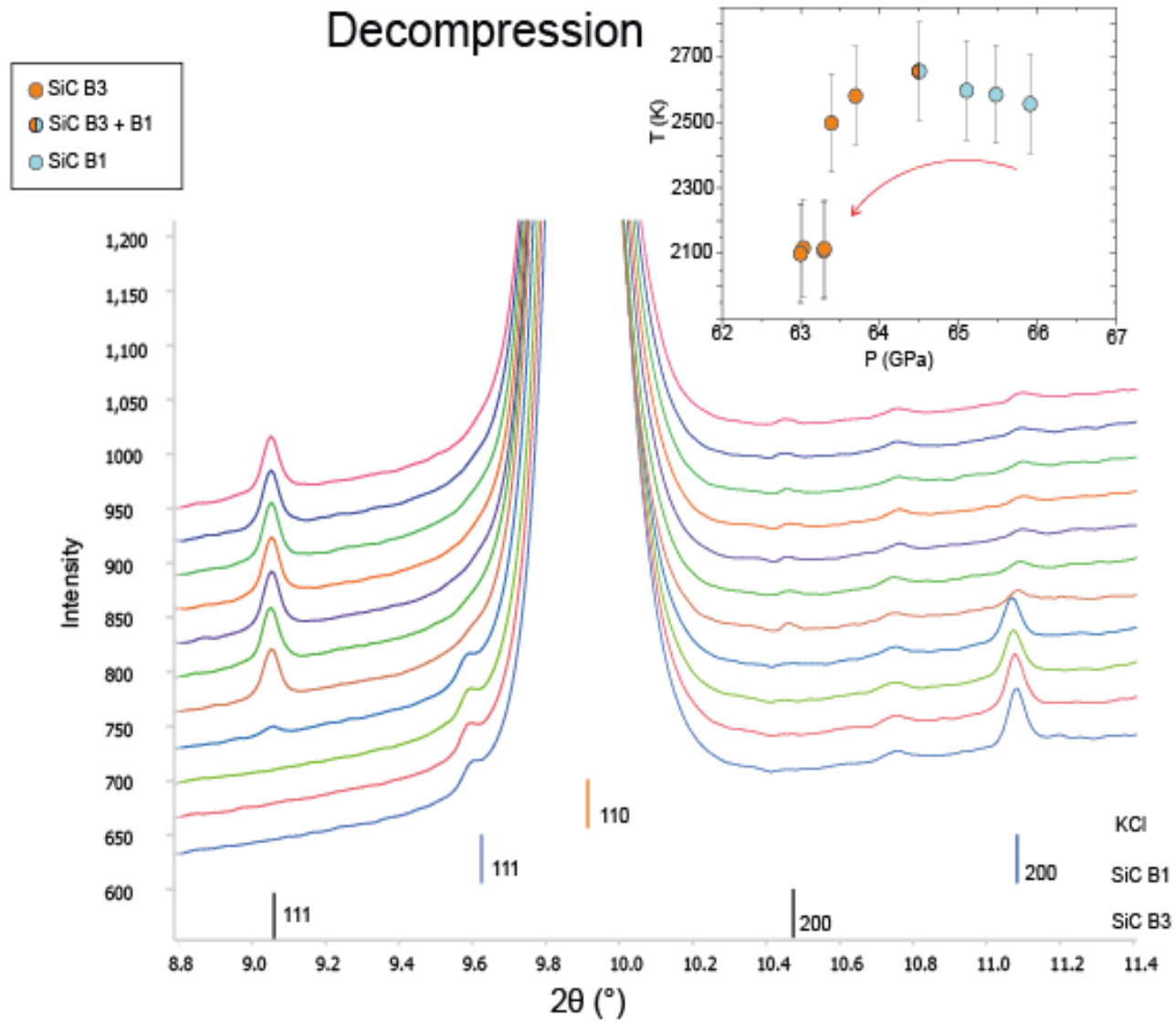
First order phase transition



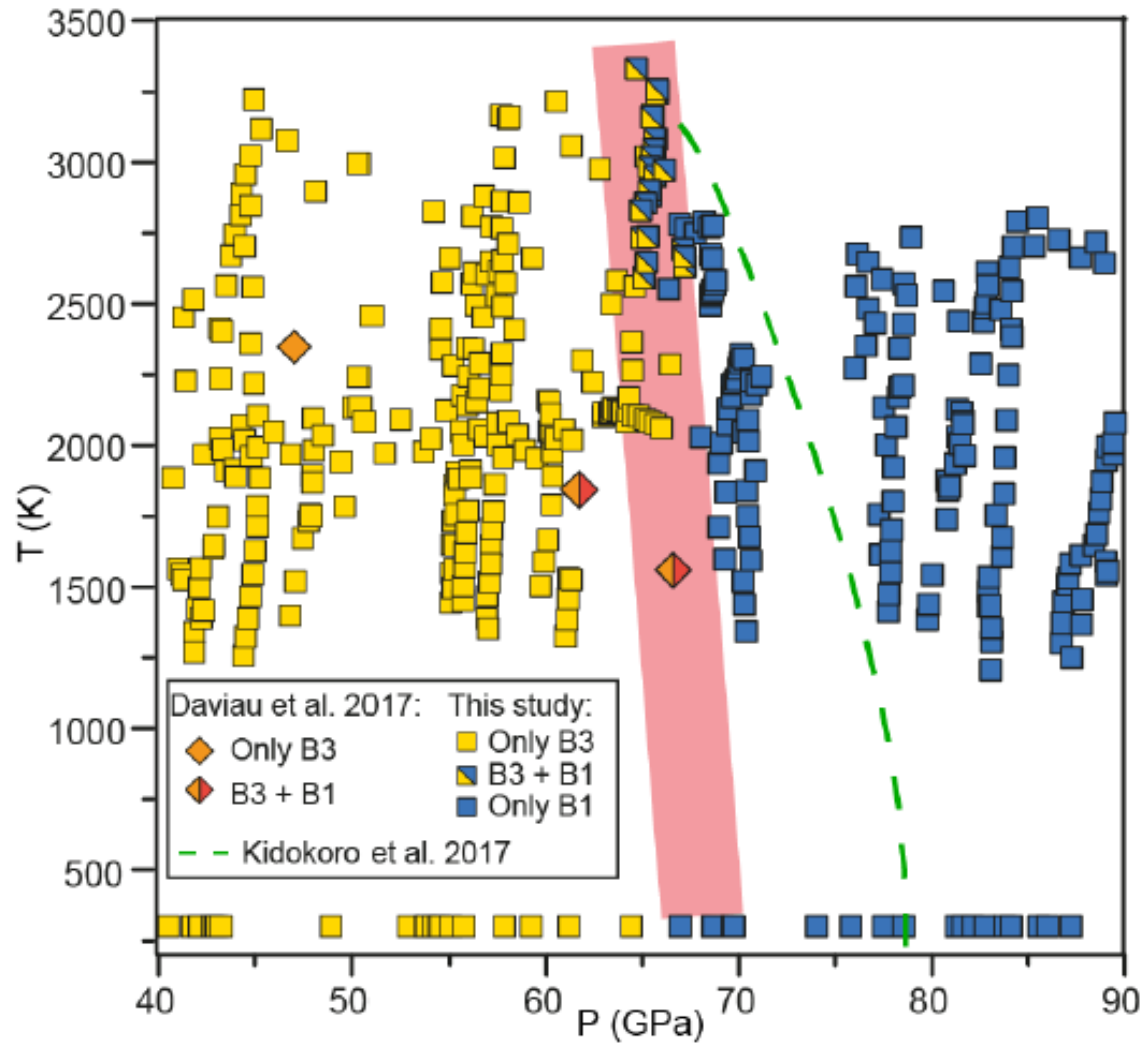
Potential existence of carbide exoplanets: Interest for SiC compound phase diagram under high pressure



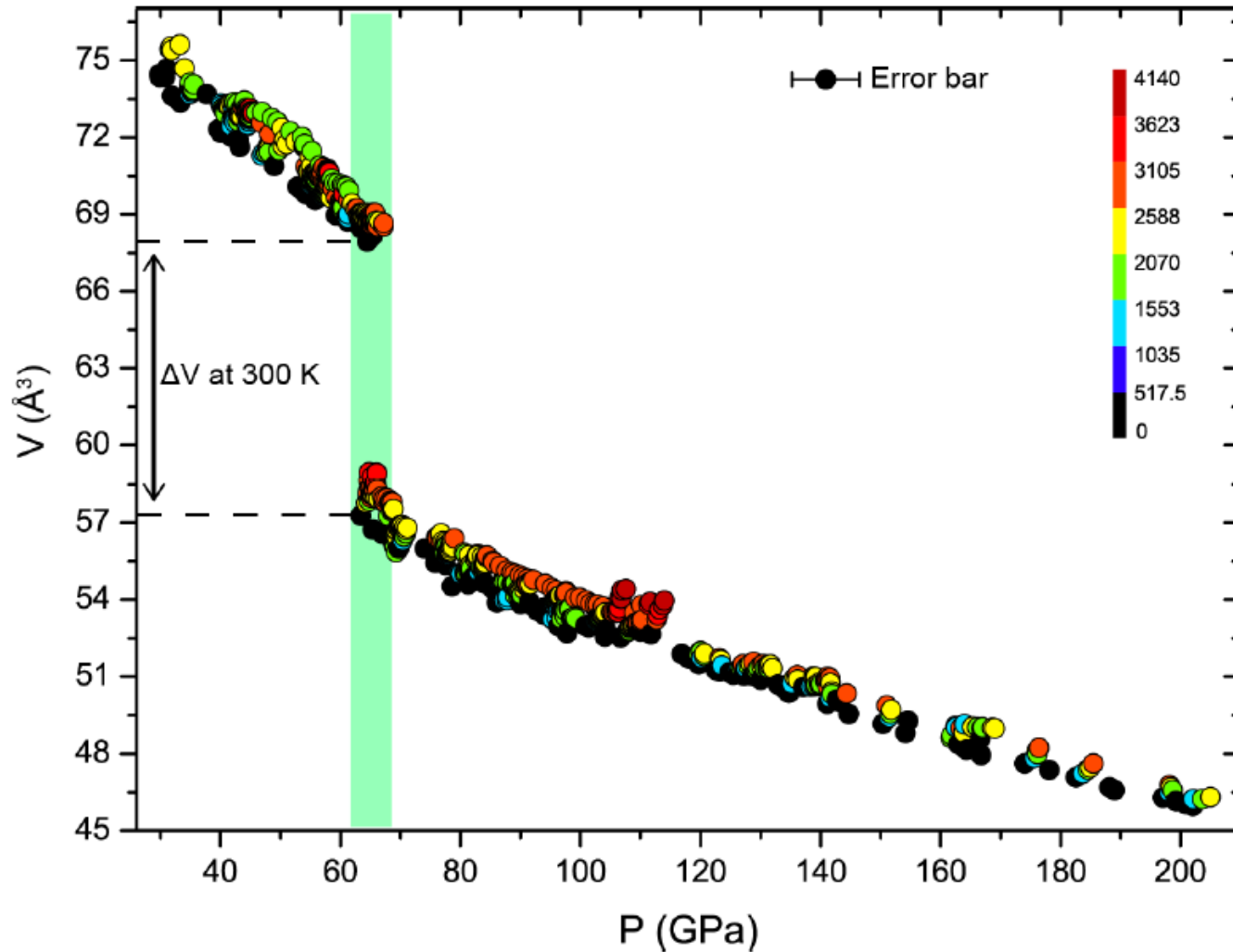
Phase transition by changing pressure at high temperature

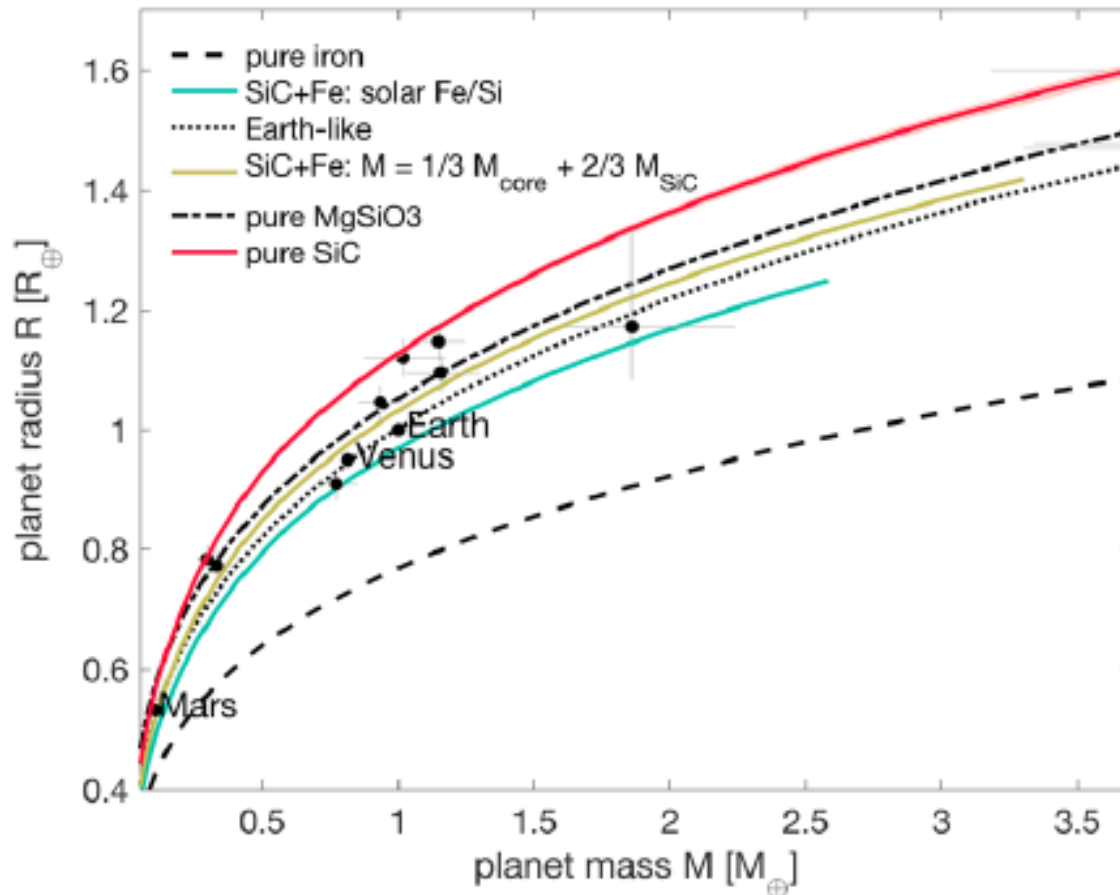


Accurate phase diagram could be then established



Change in structure is related with a large change in volume





Modeling a SiC+Fe planet

Journal of Geophysical Research: Planets

Equation of State of SiC at Extreme Conditions: New Insight Into the Interior of Carbon-Rich Exoplanets

F. Miozzi¹ , G. Morard¹ , D. Antonangeli¹ , A. N. Clark² , M. Mezouar³, C. Dorn⁴ ,
A. Rozel⁵ , and G. Fiquet¹ 

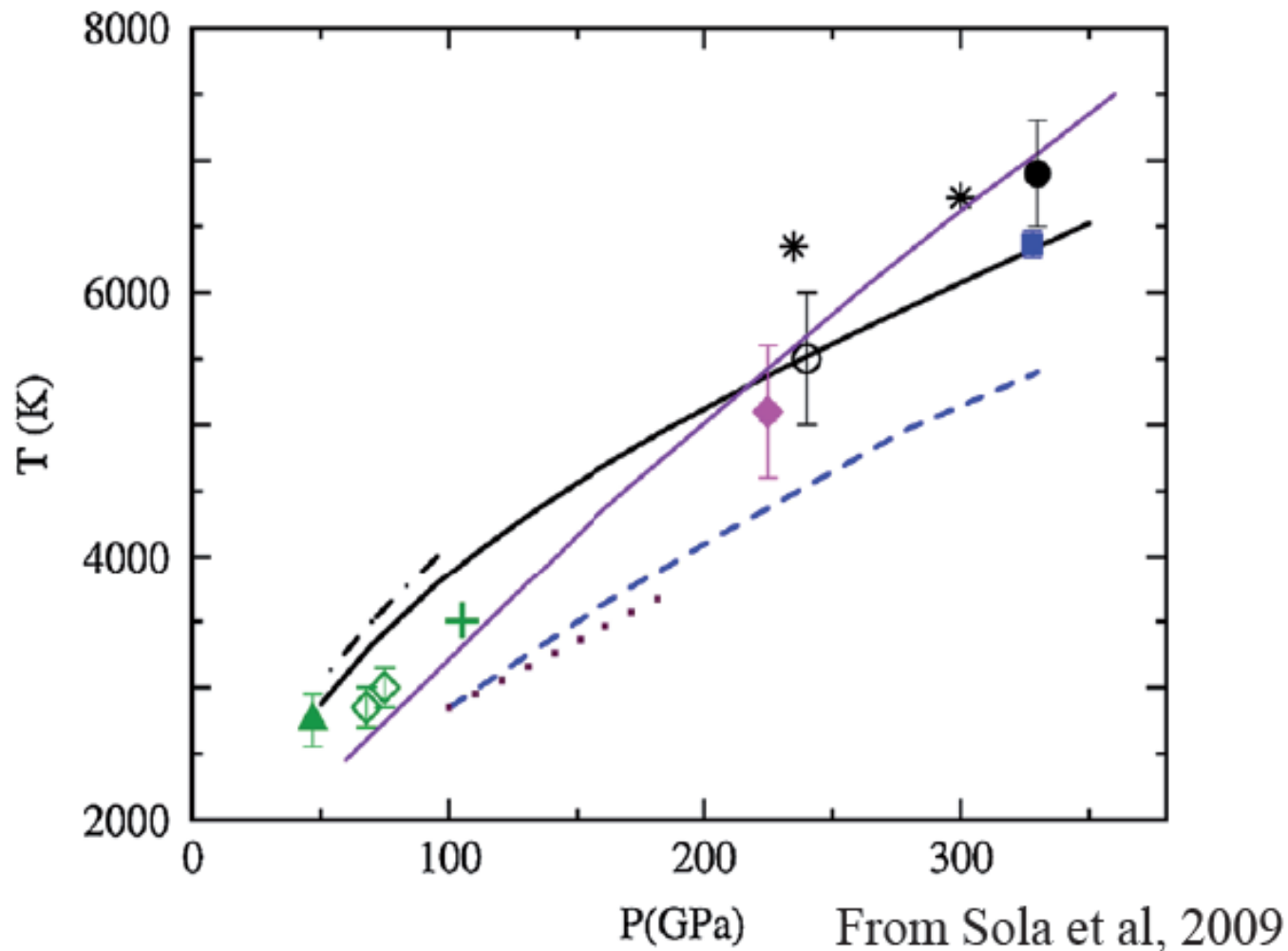
2018

Melting : congruent

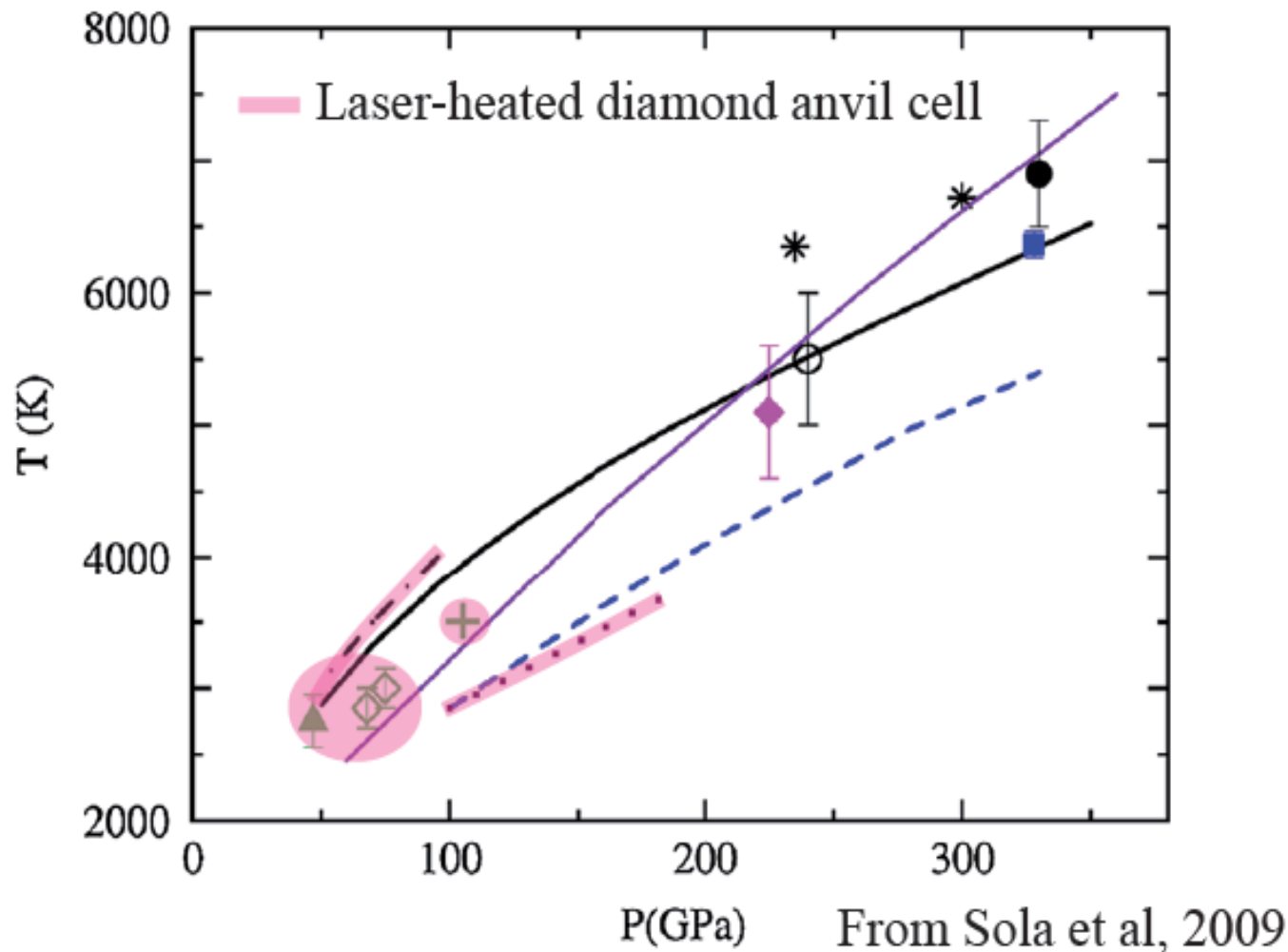
- Example of iron



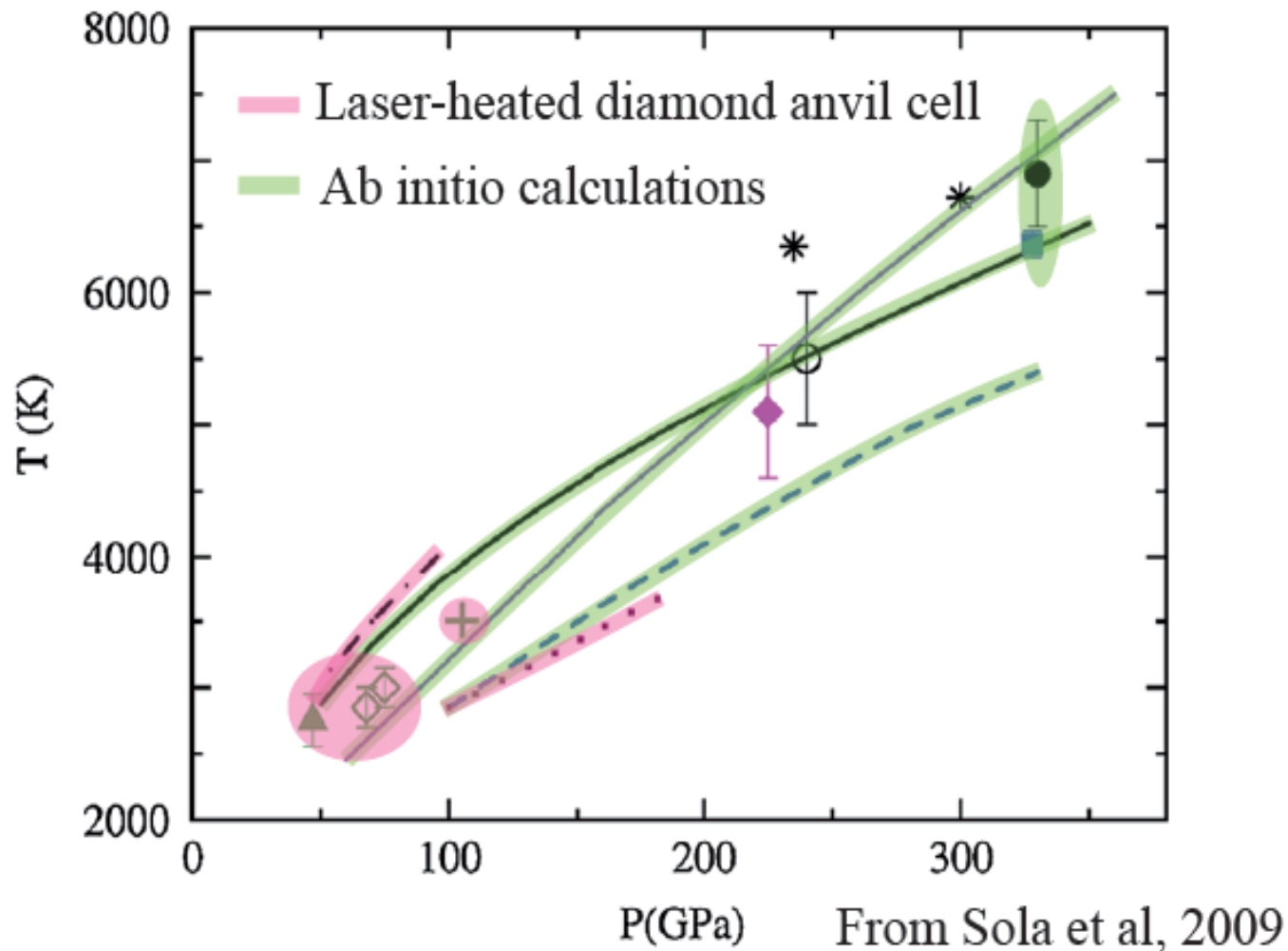
Melting of pure iron: a controversial anchoring point for the geotherm



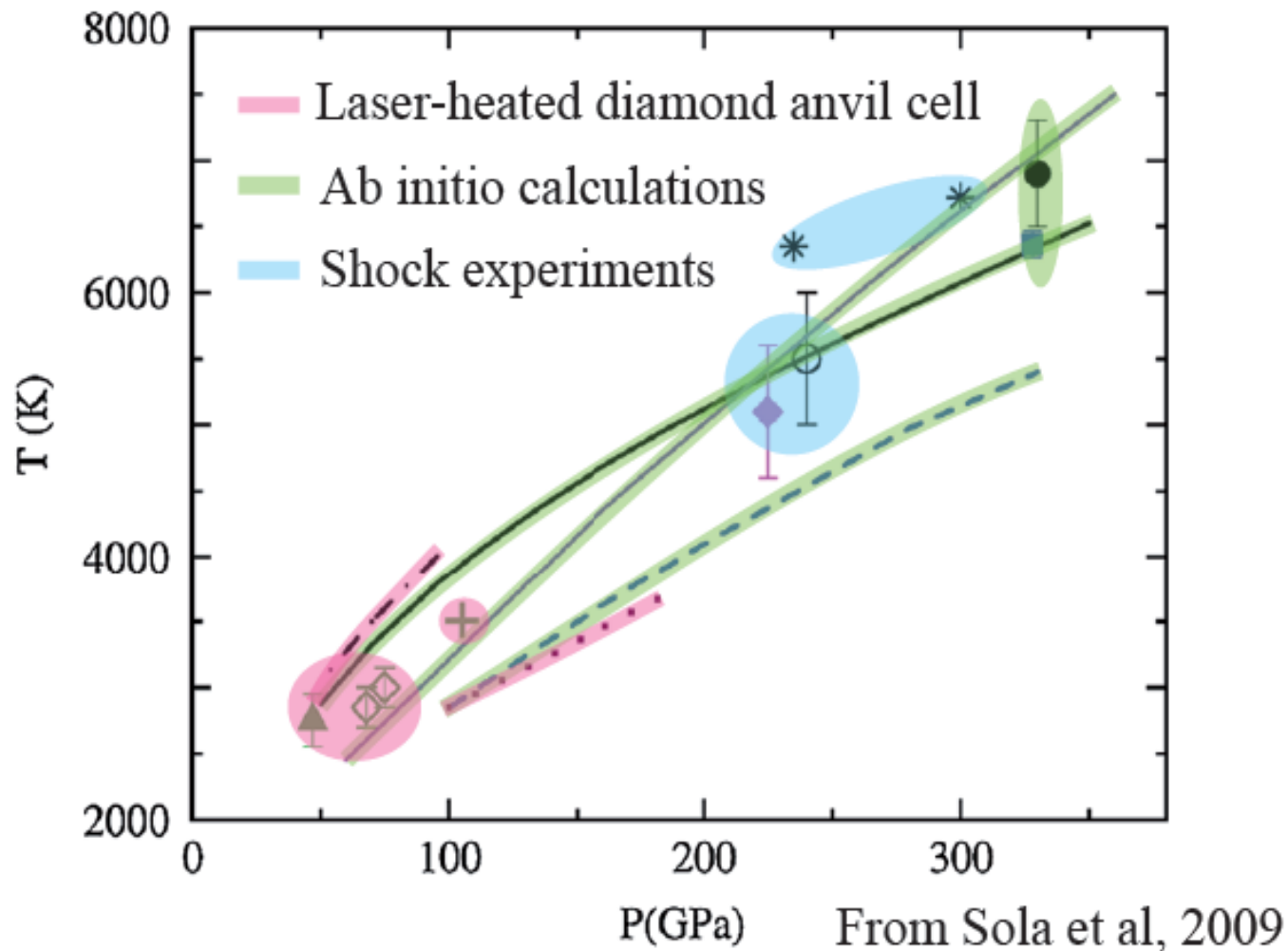
Melting of pure iron: a controversial anchoring point for the geotherm



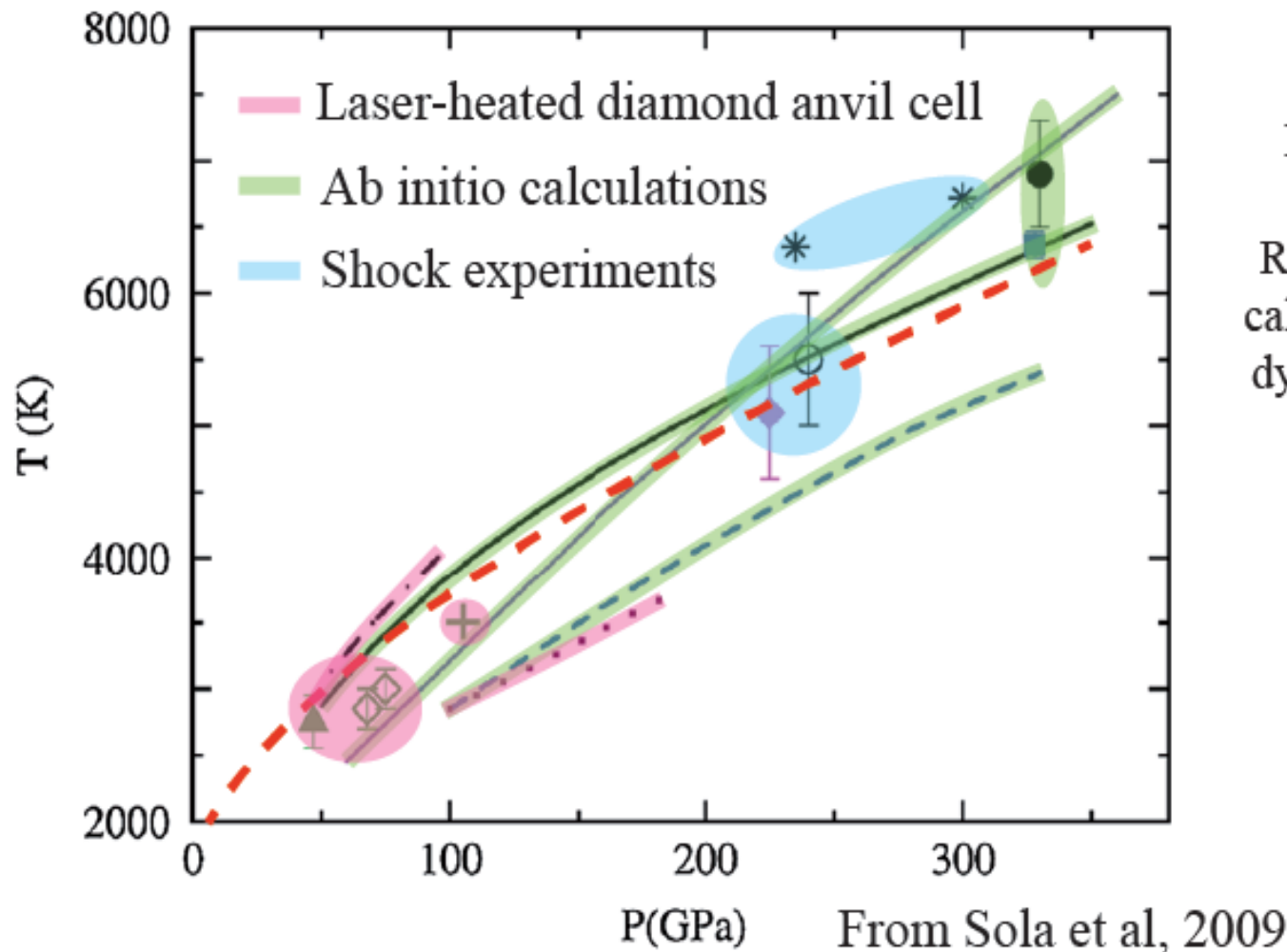
Melting of pure iron: a controversial anchoring point for the geotherm



Melting of pure iron: a controversial anchoring point for the geotherm



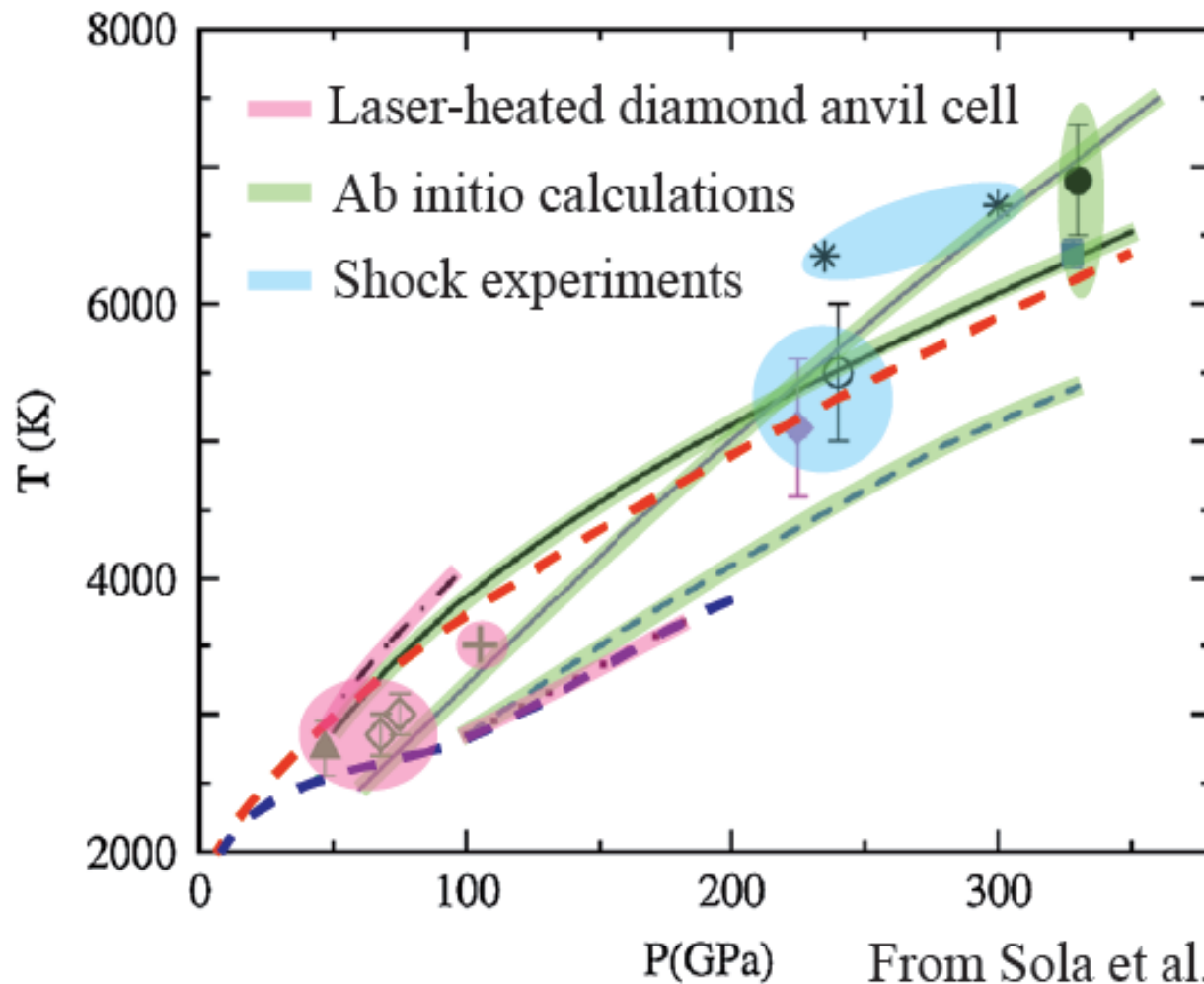
Melting of pure iron: a controversial anchoring point for the geotherm



Anzellini et al,
Science, 2013

In situ XRD study
Diffuse scattering
Reconciling ab initio
calculations, static and
dynamic compression

Melting of pure iron: a controversial anchoring point for the geotherm



Anzellini et al,
Science, 2013

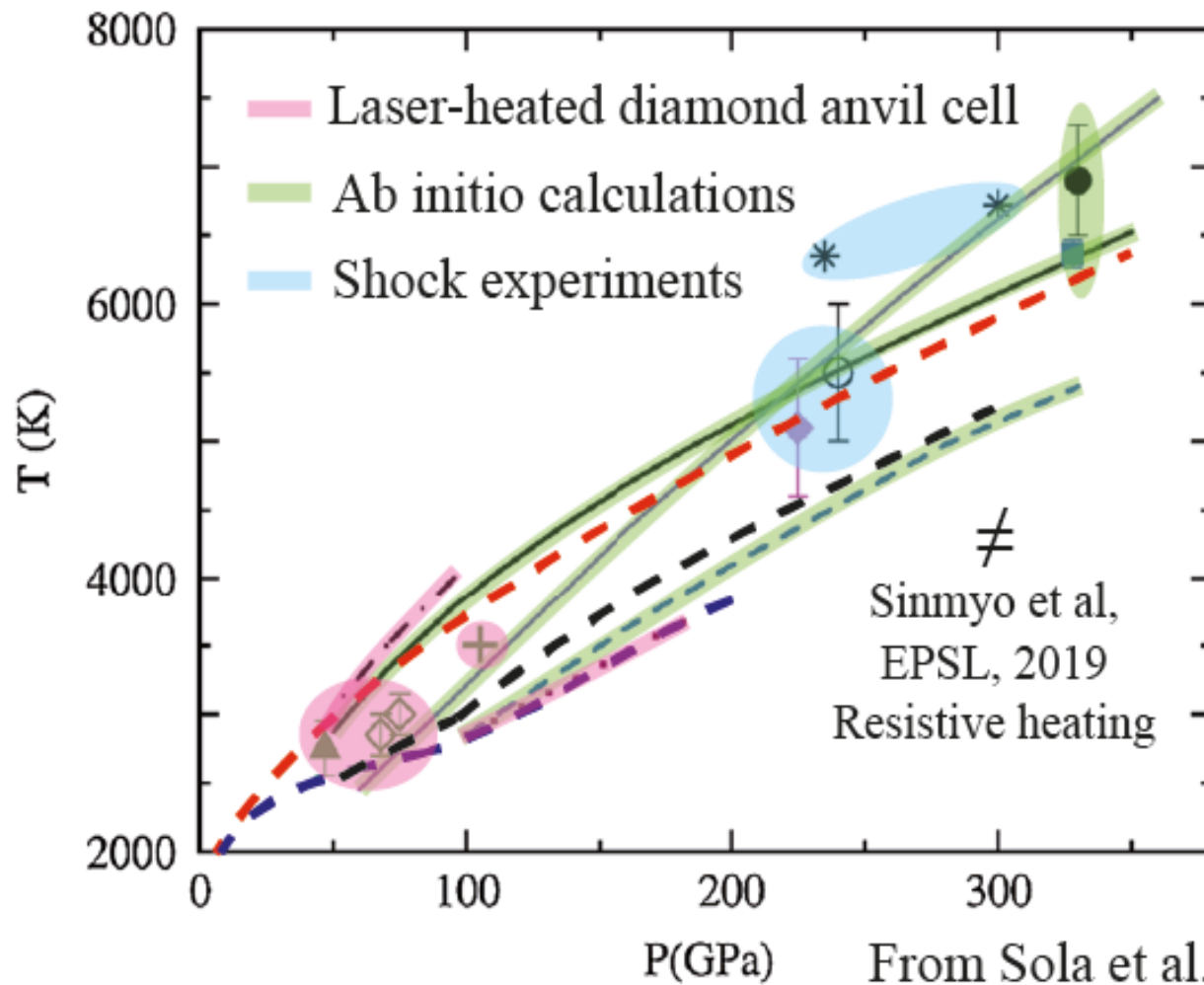
In situ XRD study
Diffuse scattering
Reconciling ab initio
calculations, static and
dynamic compression

≠

Aquilanti et al,
PNAS, 2015

In situ XANES study
Back on Boehler, 1993

Melting of pure iron: a controversial anchoring point for the geotherm



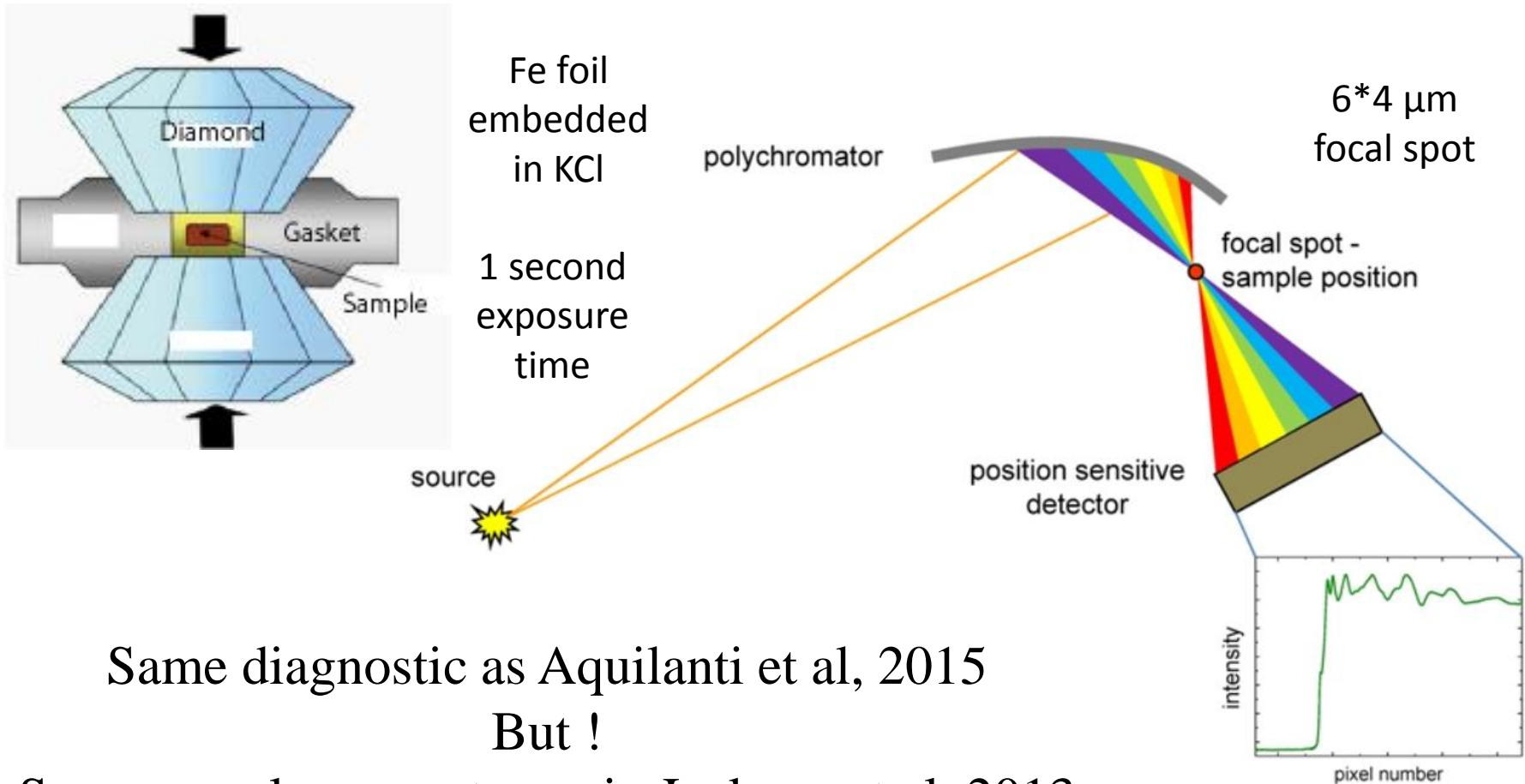
Anzellini et al,
Science, 2013

In situ XRD study
Diffuse scattering
Reconciling ab initio
calculations, static and
dynamic compression

≠
Aquilanti et al,
PNAS, 2015

In situ XANES study
Back on Boehler, 1993

Energy dispersive EXAFS experimental set-up coupled with Laser-Heated Diamond Anvil Cell on ID24 beamline, ESRF

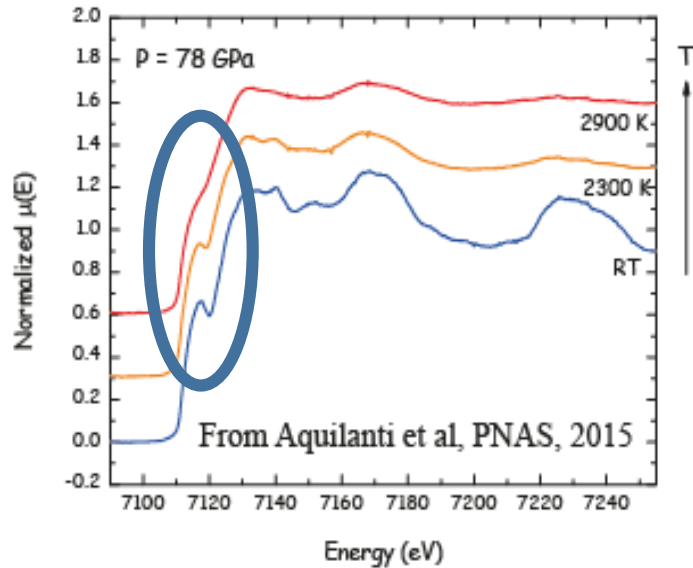


Same diagnostic as Aquilanti et al, 2015

But !

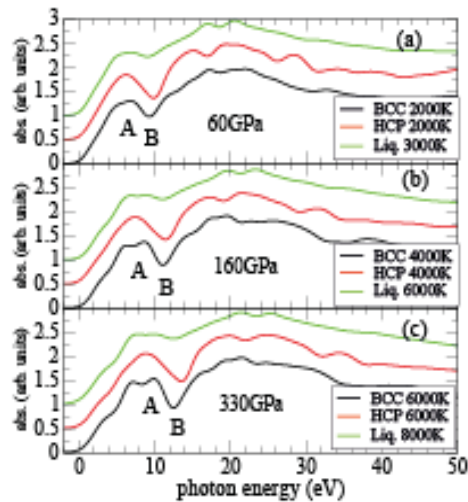
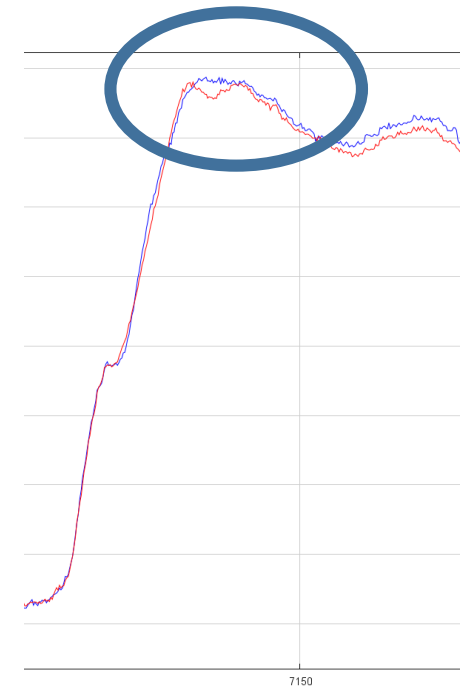
Same sample geometry as in Jackson et al, 2013
and Anzellini et al, 2013

In situ criteria for XANES experiments



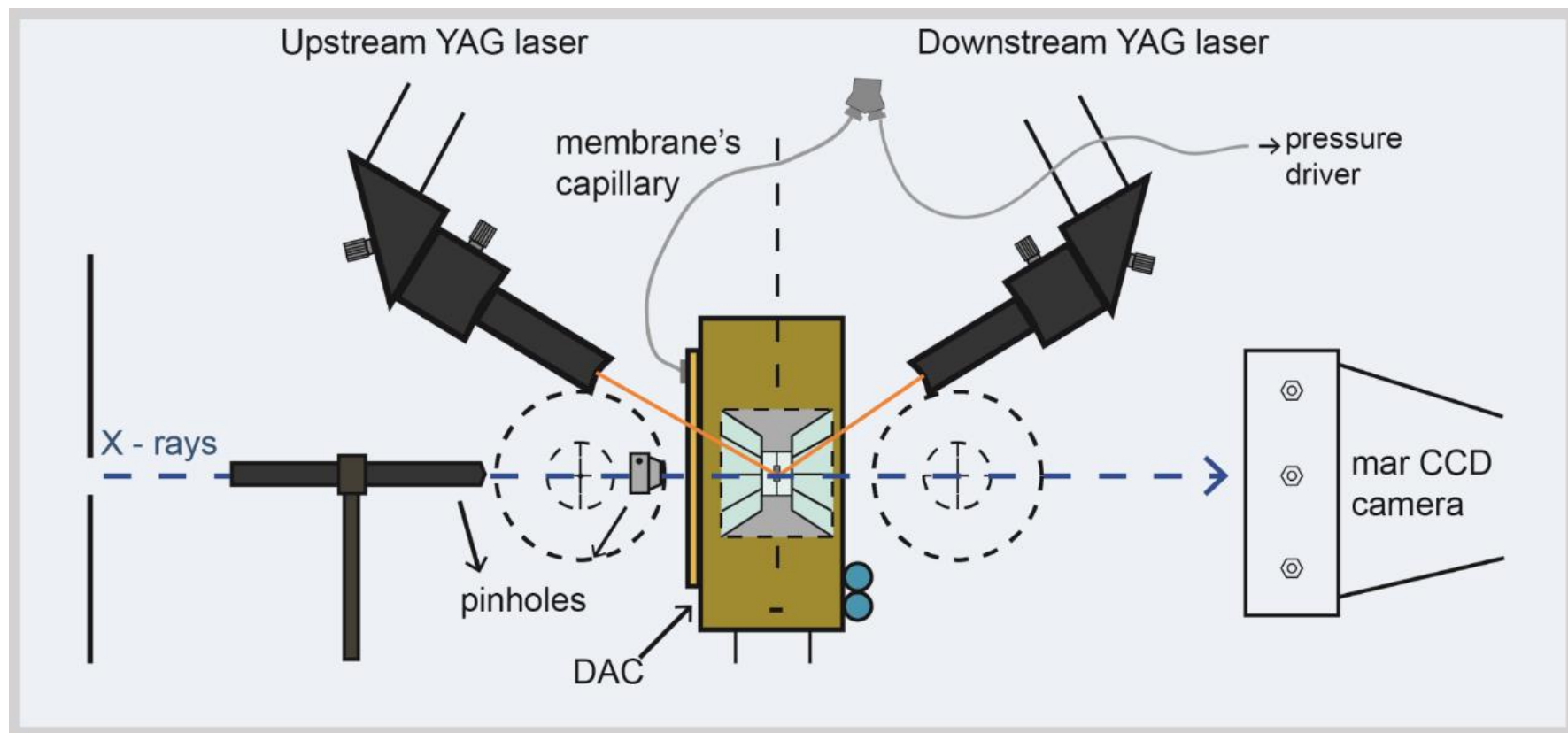
Change of
the edge
upon
melting

hcp-fcc
transition

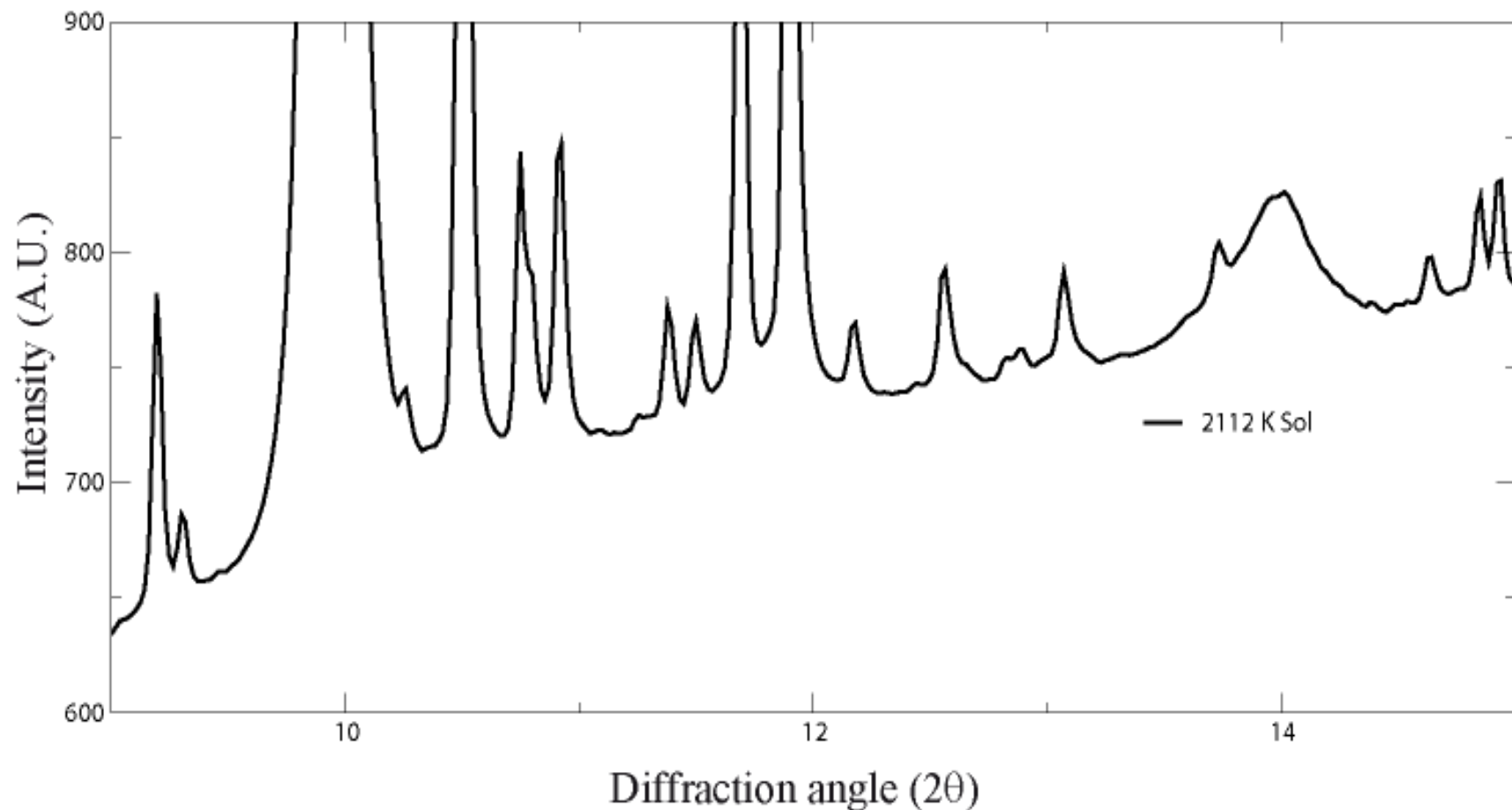


From Mazevet et al, Phys. Rev B, 2014

In situ X-ray diffraction on ID27

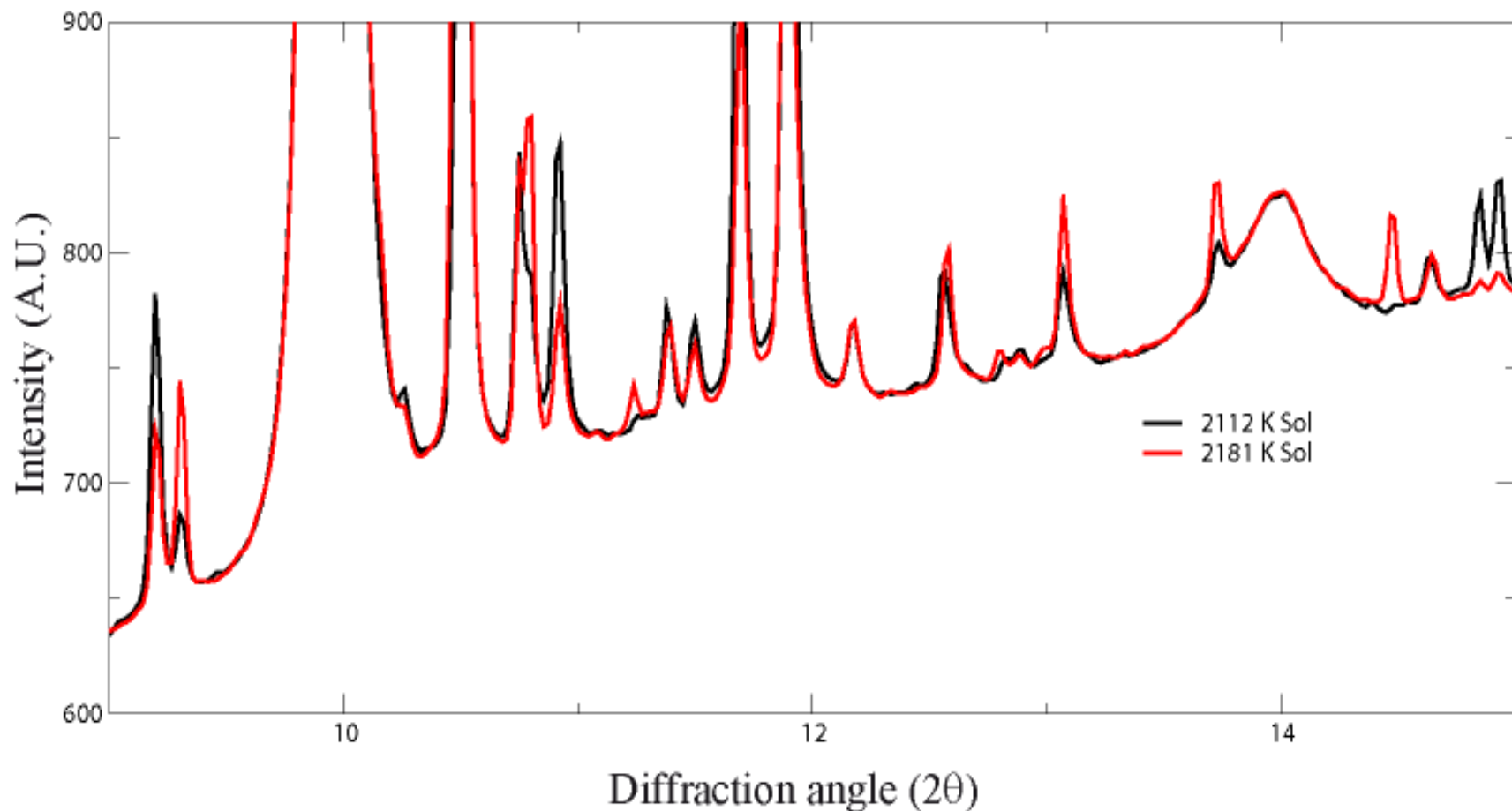


In situ detection of melting in LHDAC



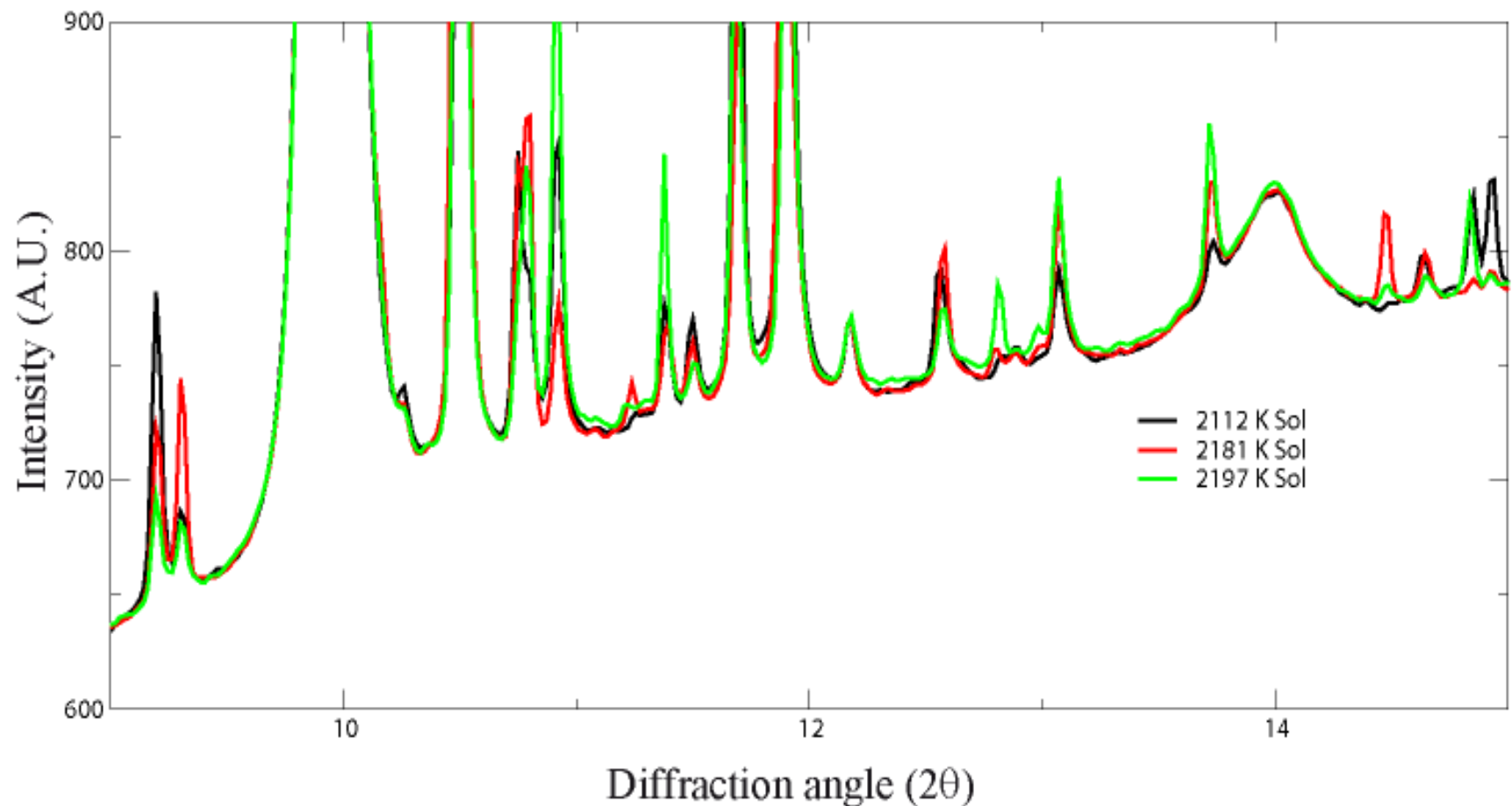
Fe-5wt% Ni-12wt% S ; P~67 GPa

In situ detection of melting in LHDAC



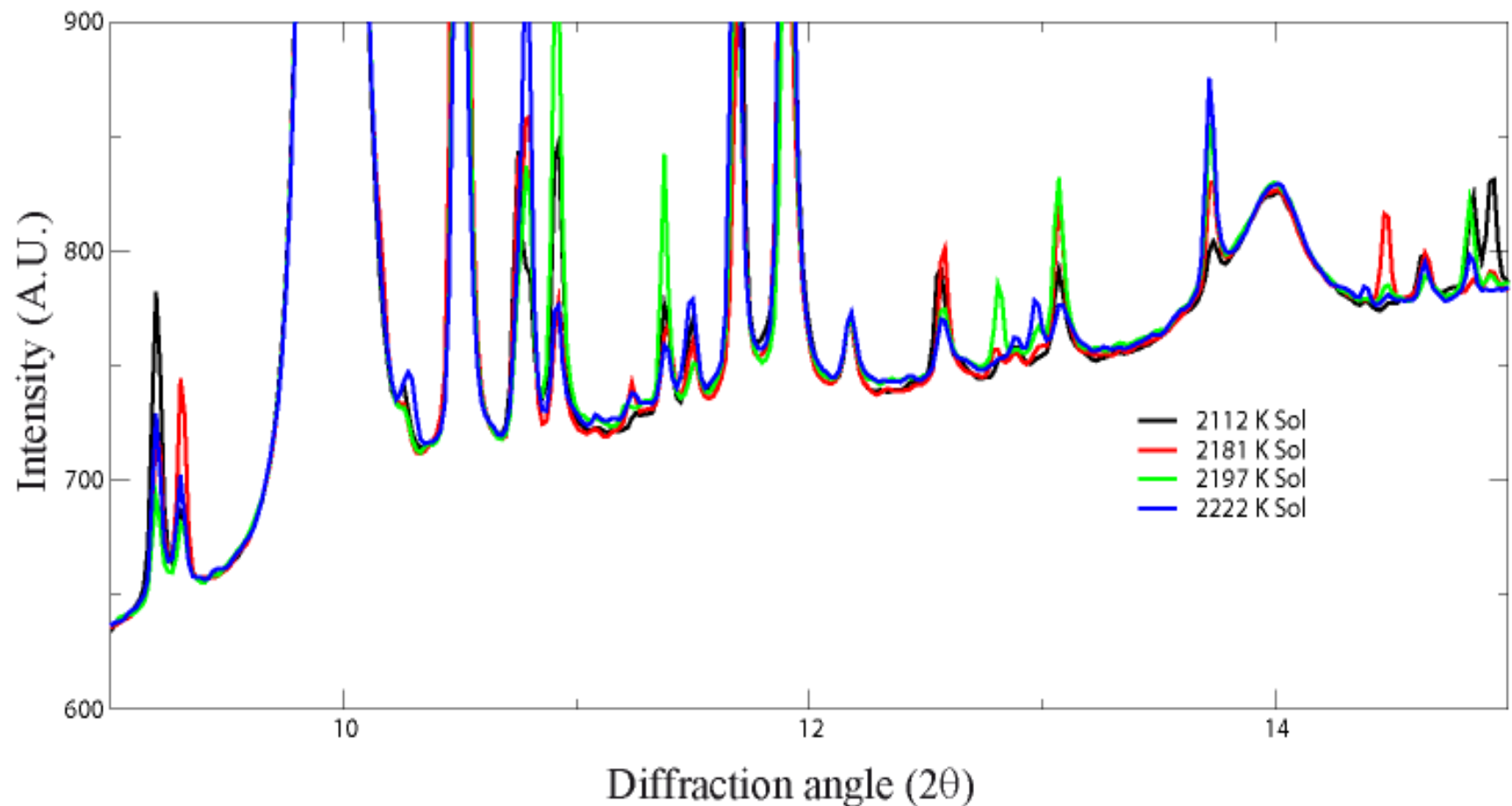
Fe-5wt% Ni-12wt% S ; P~67 GPa

In situ detection of melting in LHDAC



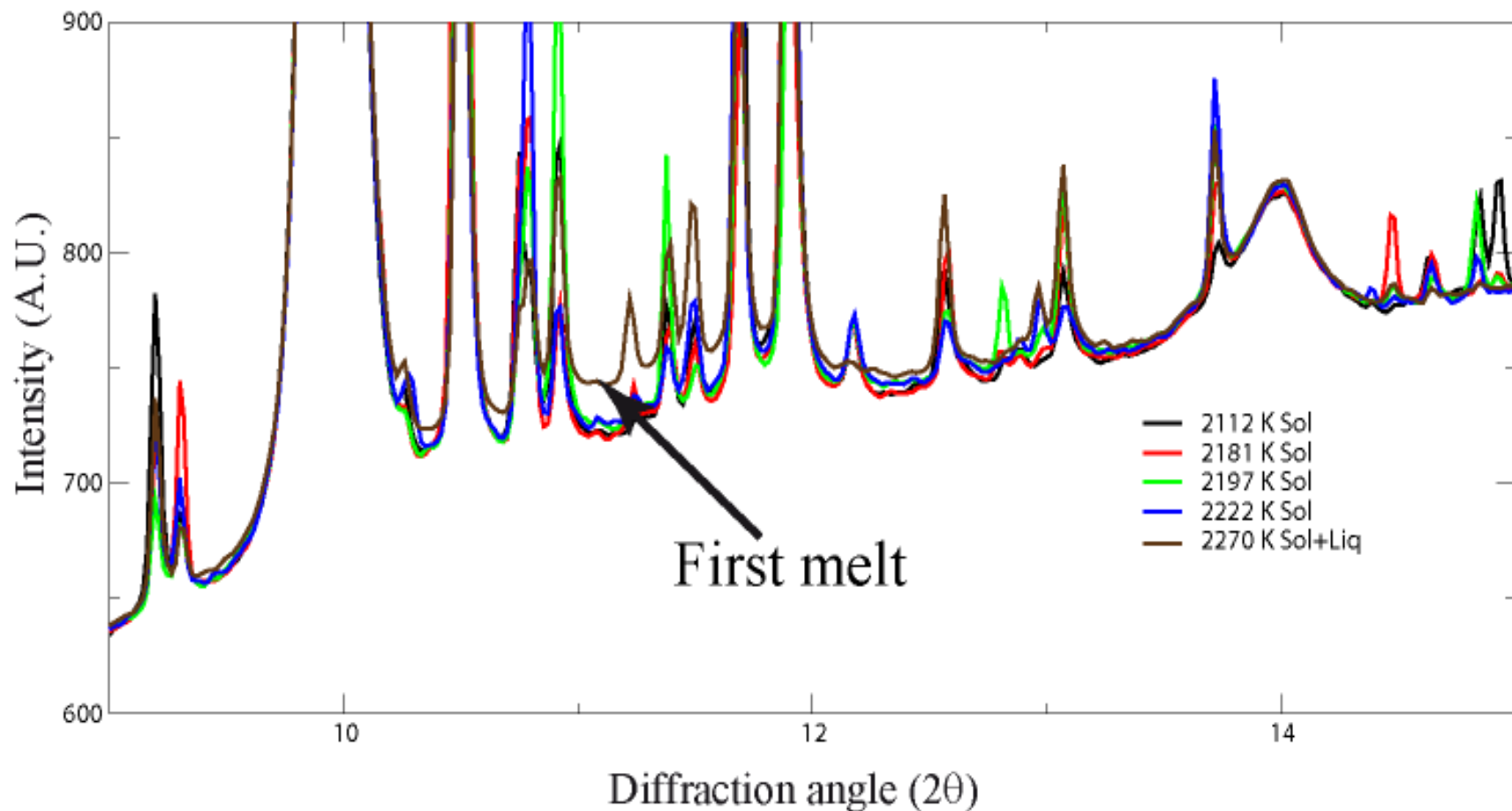
Fe-5wt% Ni-12wt% S ; P~67 GPa

In situ detection of melting in LHDAC



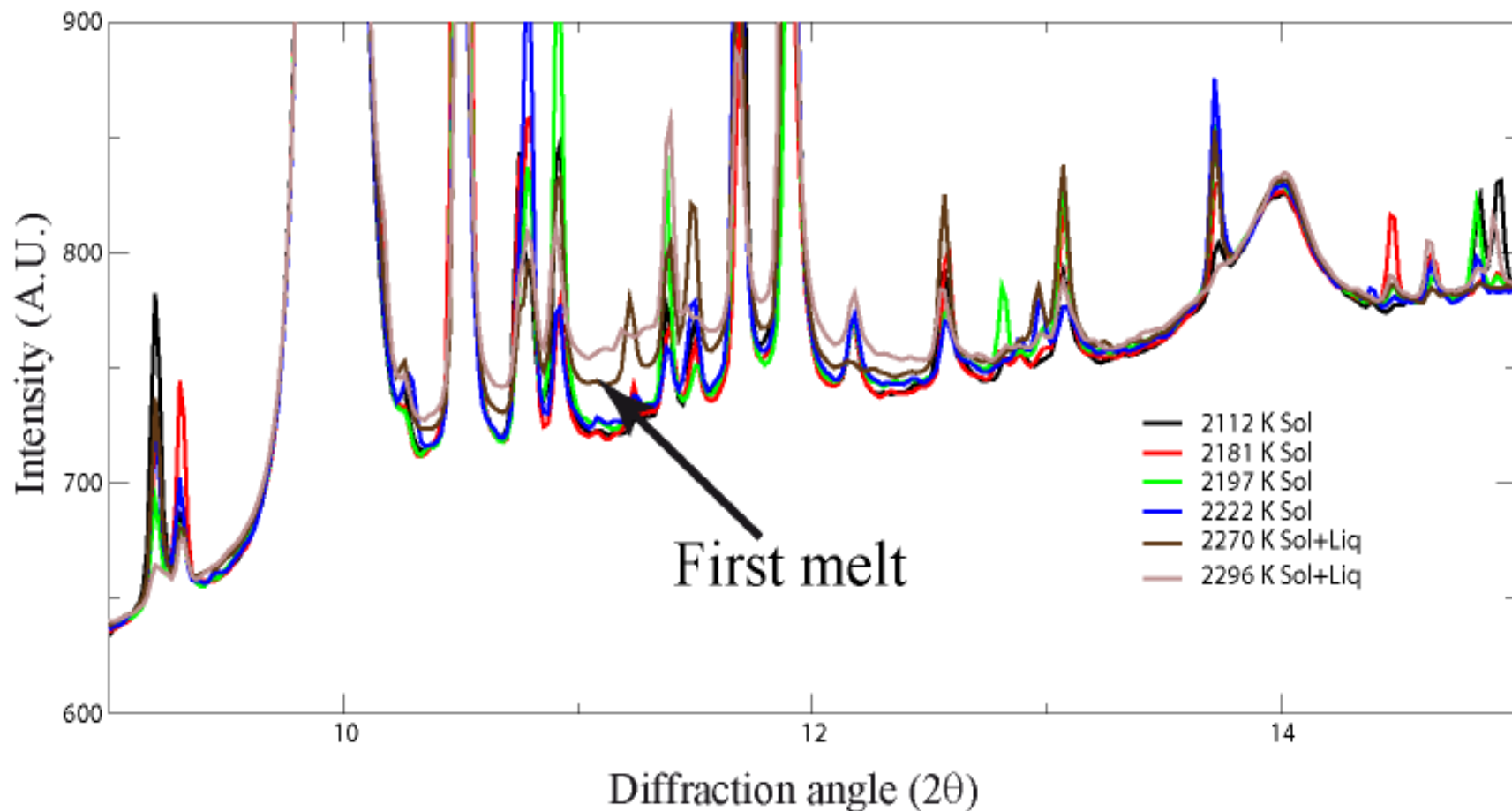
Fe-5wt% Ni-12wt% S ; P~67 GPa

In situ detection of melting in LHDAC



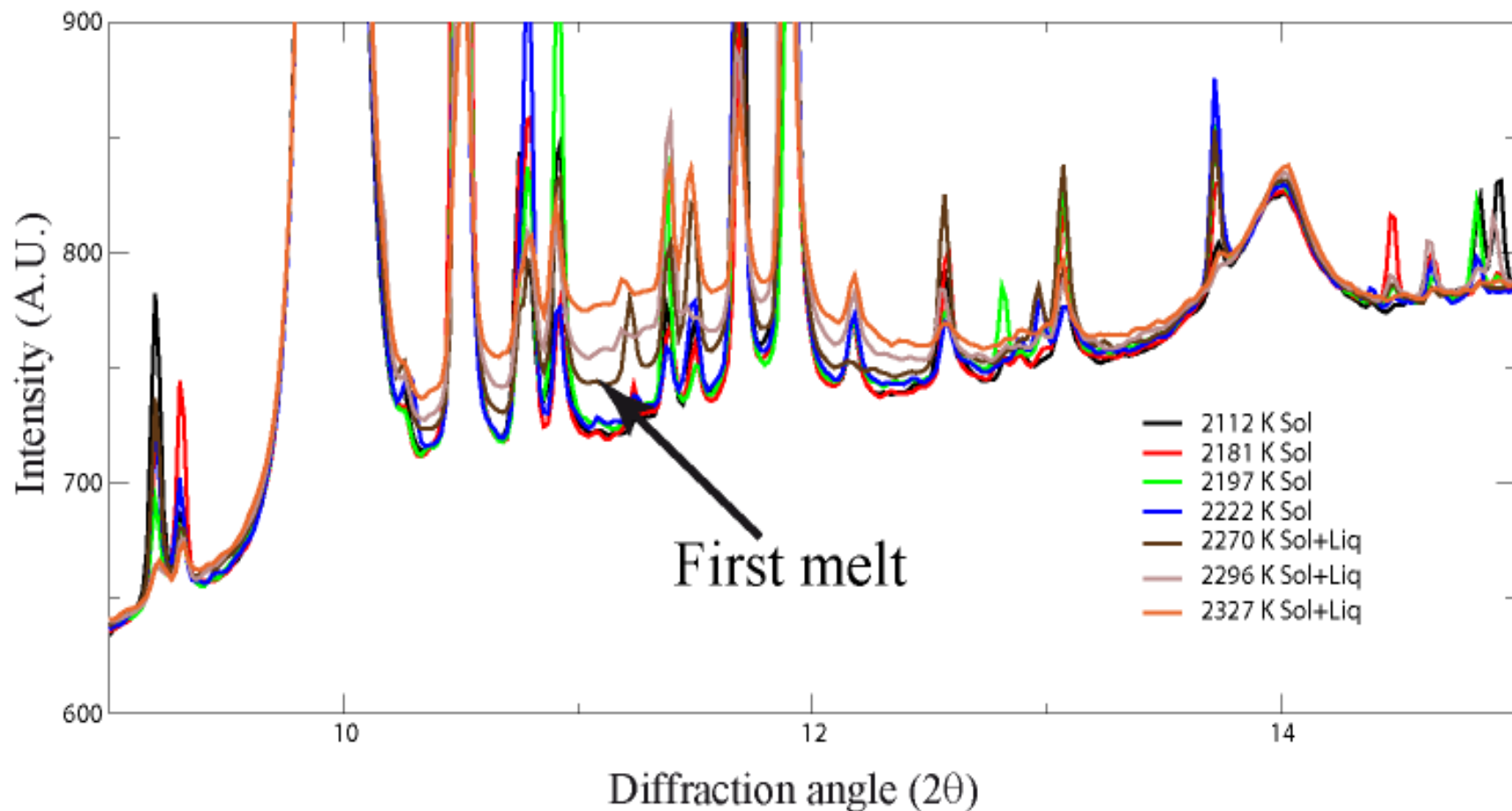
Fe-5wt% Ni-12wt% S ; P~67 GPa

In situ detection of melting in LHDAC



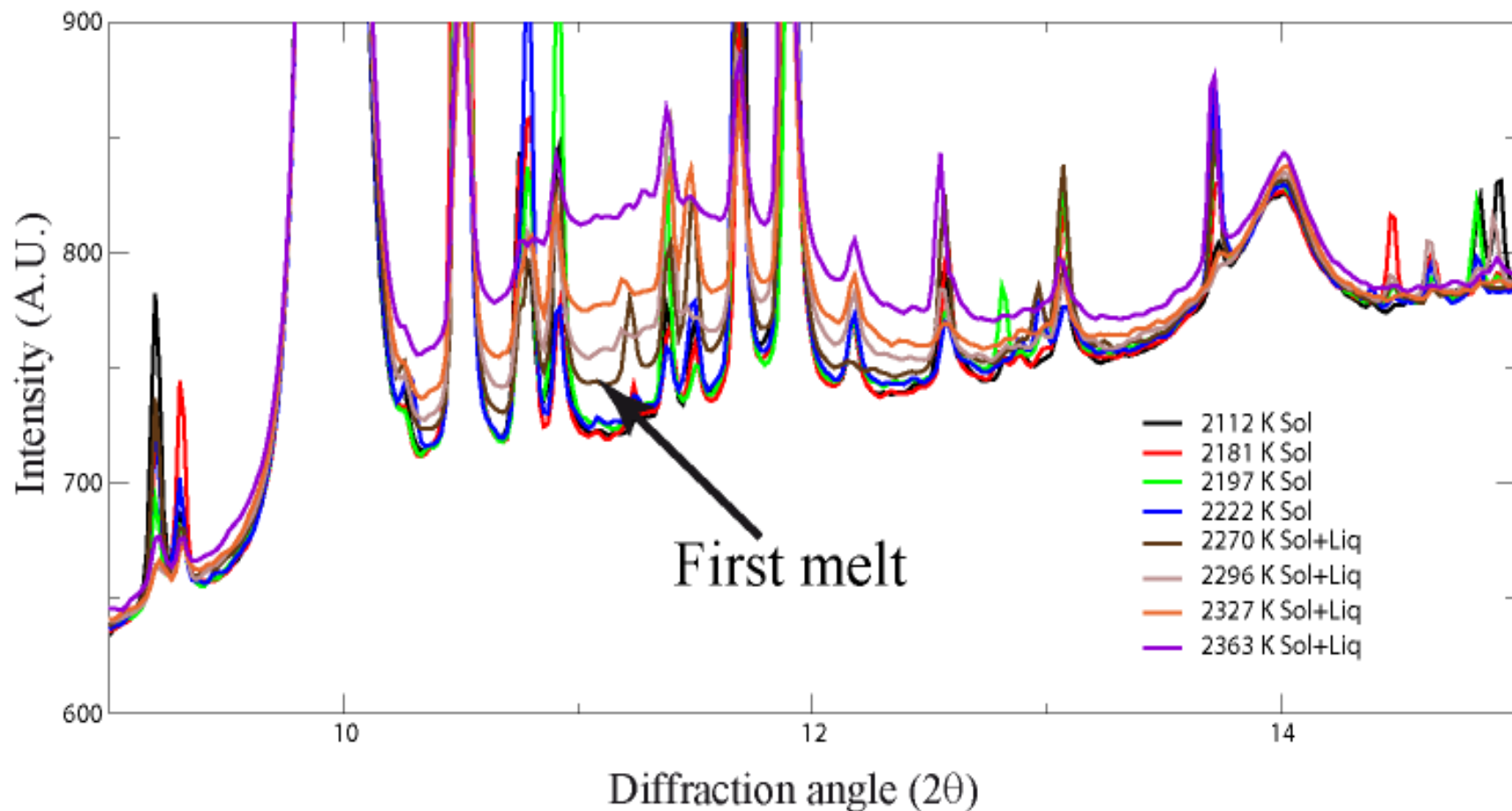
Fe-5wt% Ni-12wt% S ; P~67 GPa

In situ detection of melting in LHDAC



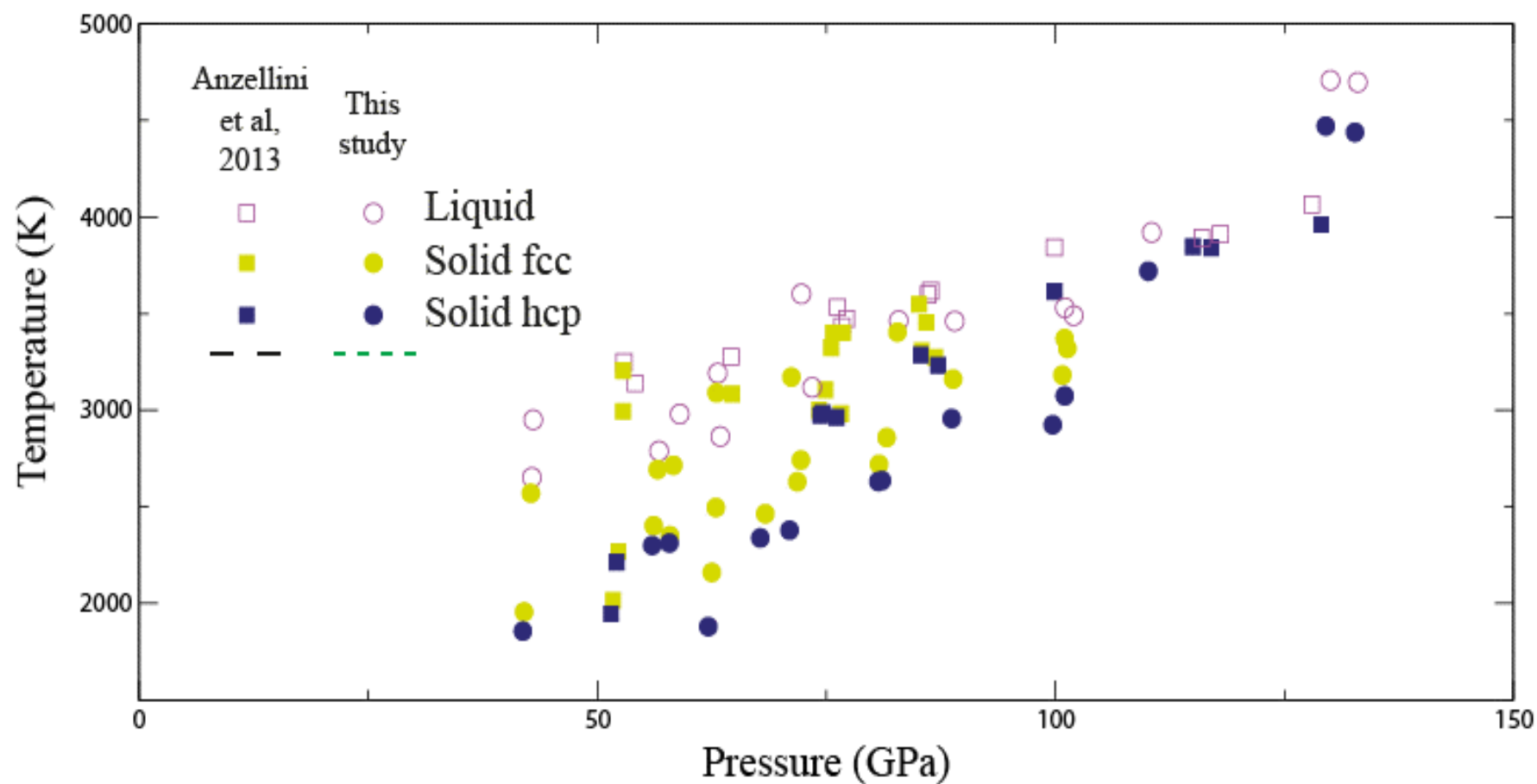
Fe-5wt% Ni-12wt% S ; P~67 GPa

In situ detection of melting in LHDAC

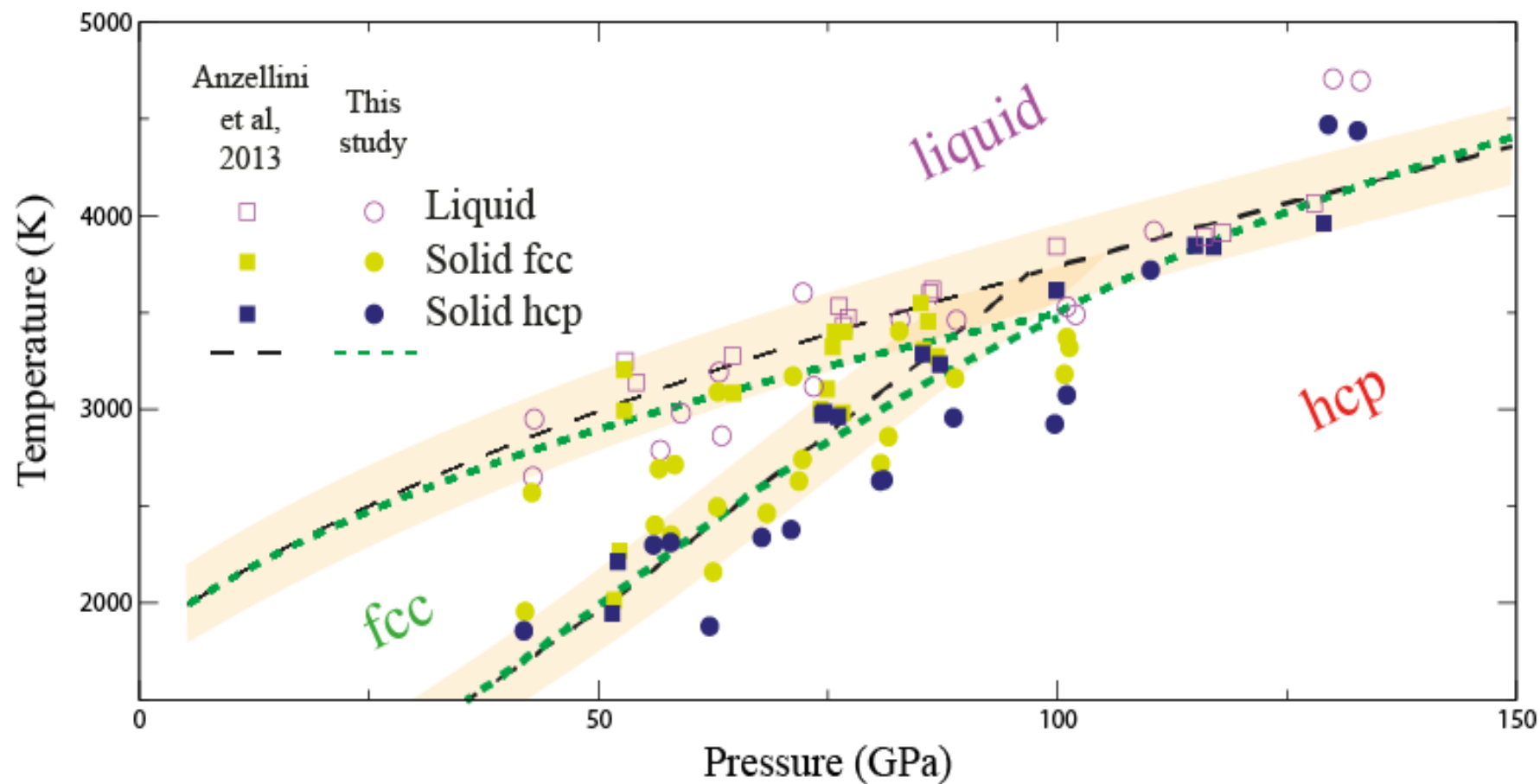


Fe-5wt% Ni-12wt% S ; P~67 GPa

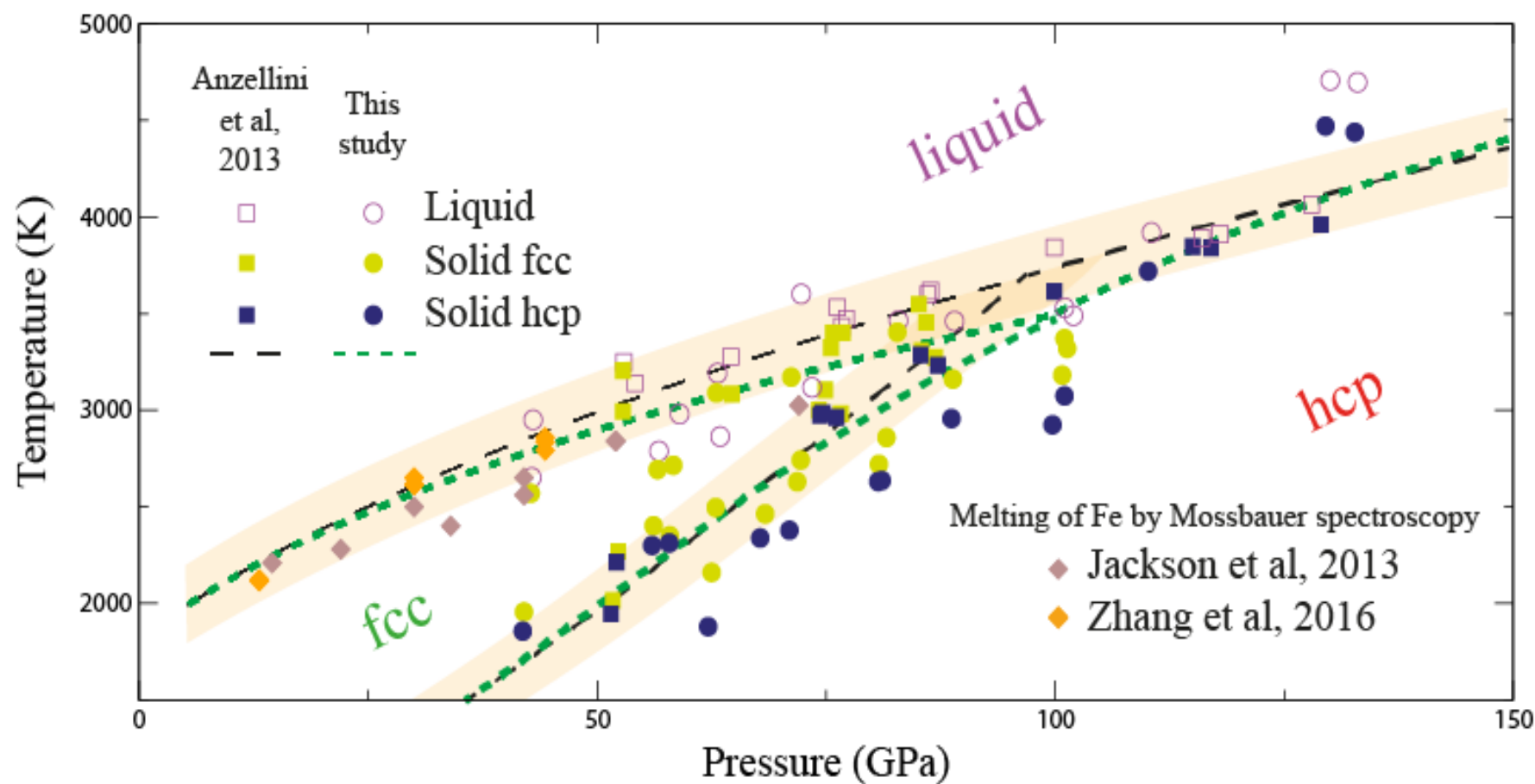
Comparison with previous studies



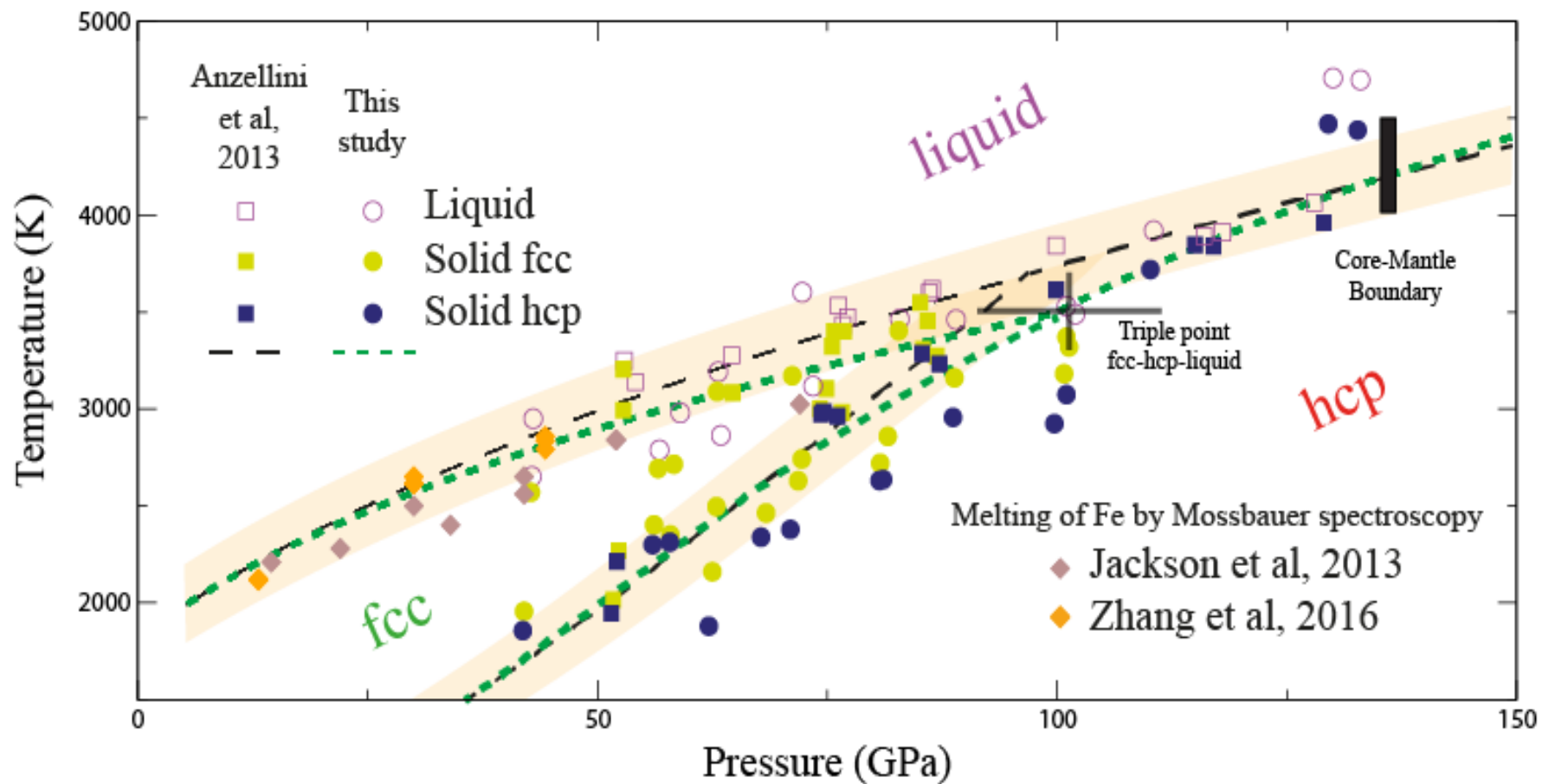
Comparison with previous studies



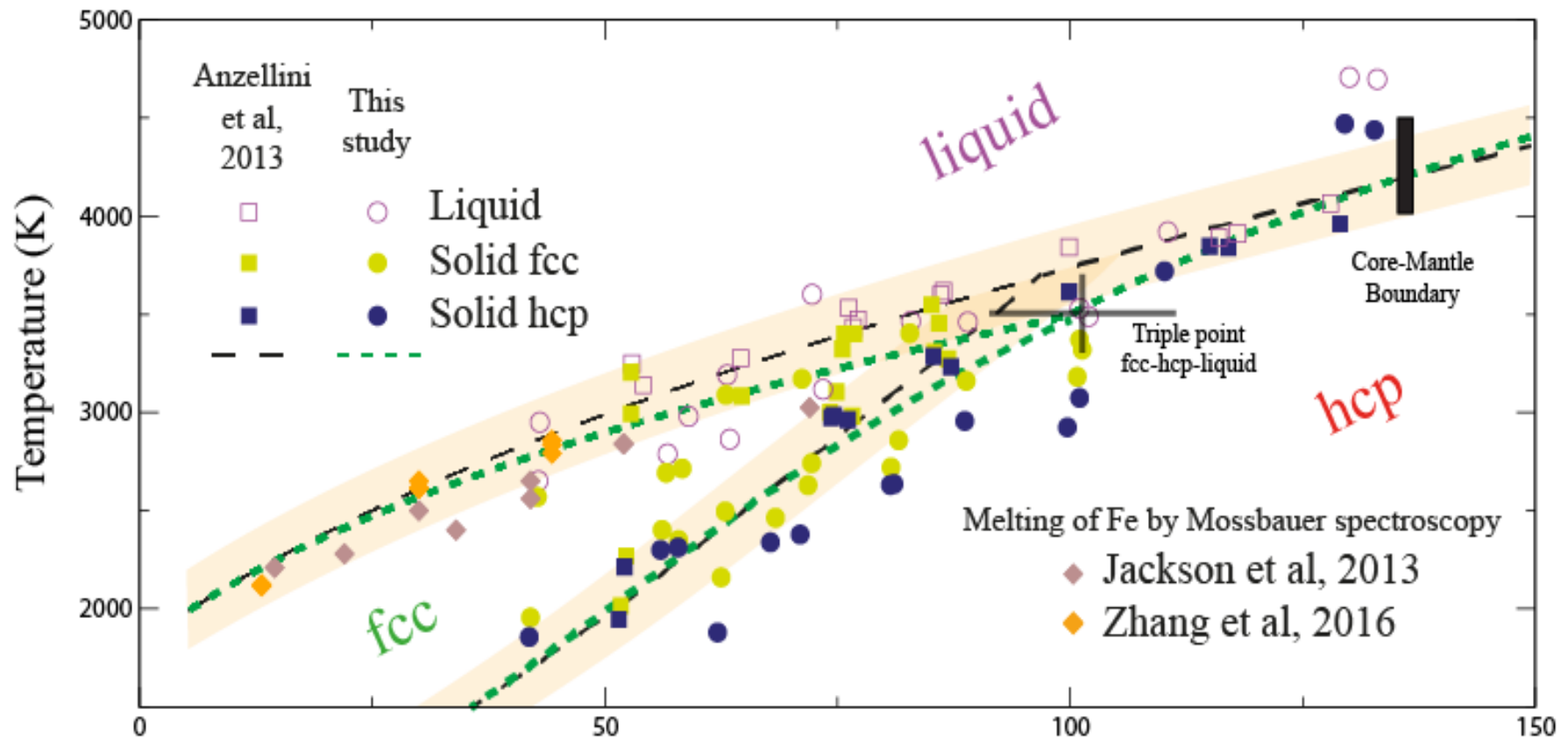
Comparison with previous studies



Comparison with previous studies










Comparison with previous studies

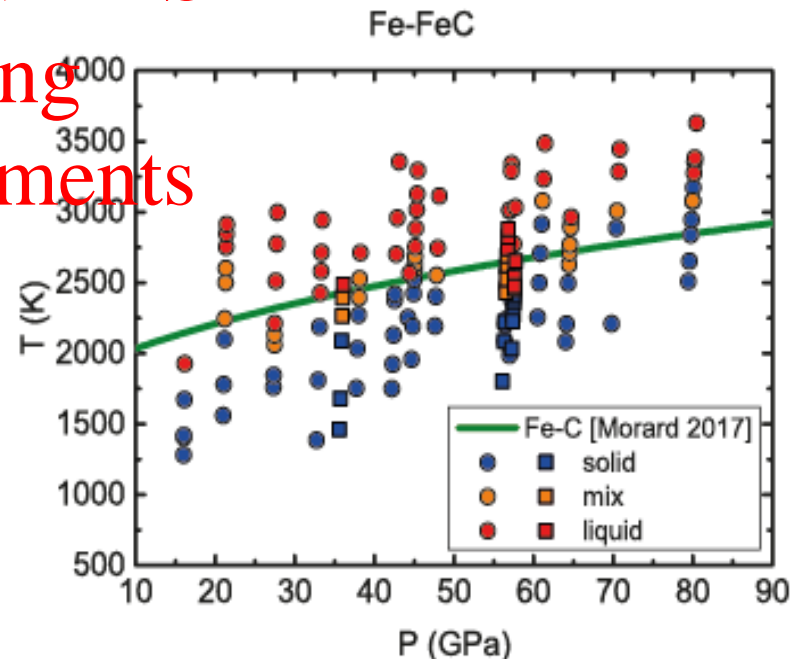
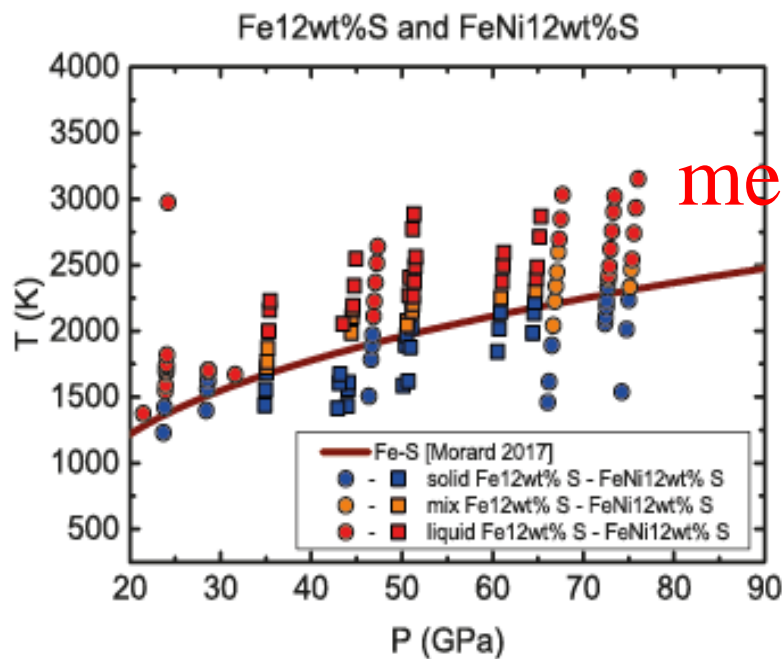
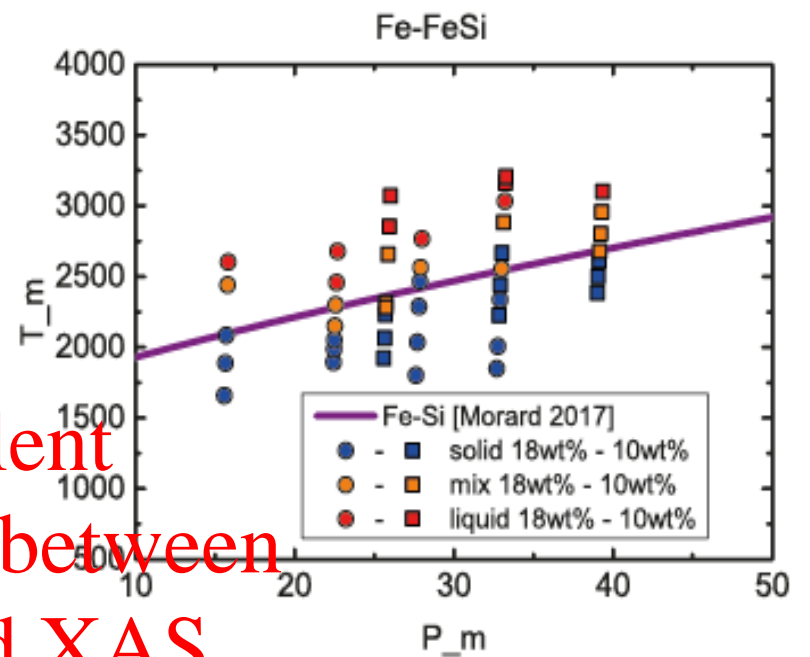
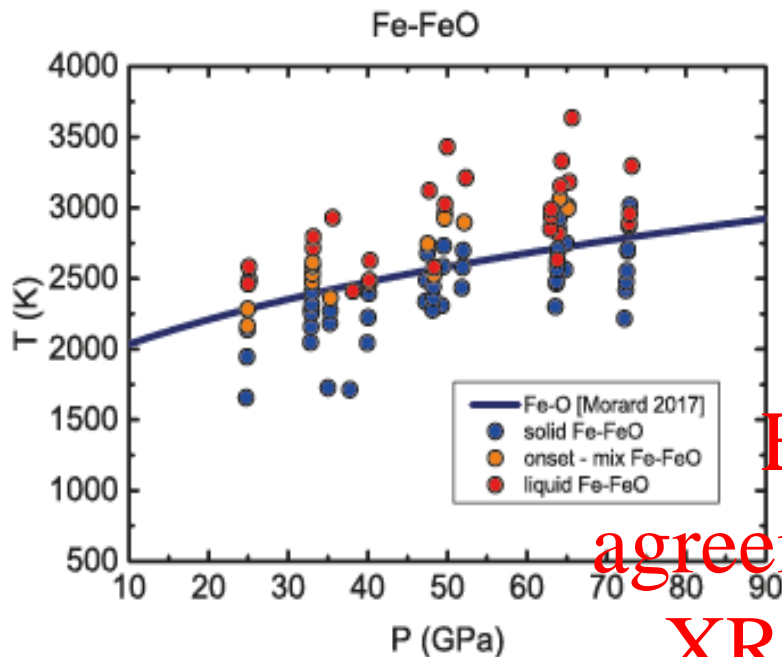


Solving Controversies on the Iron Phase Diagram Under High Pressure

Geophysical Research Letters

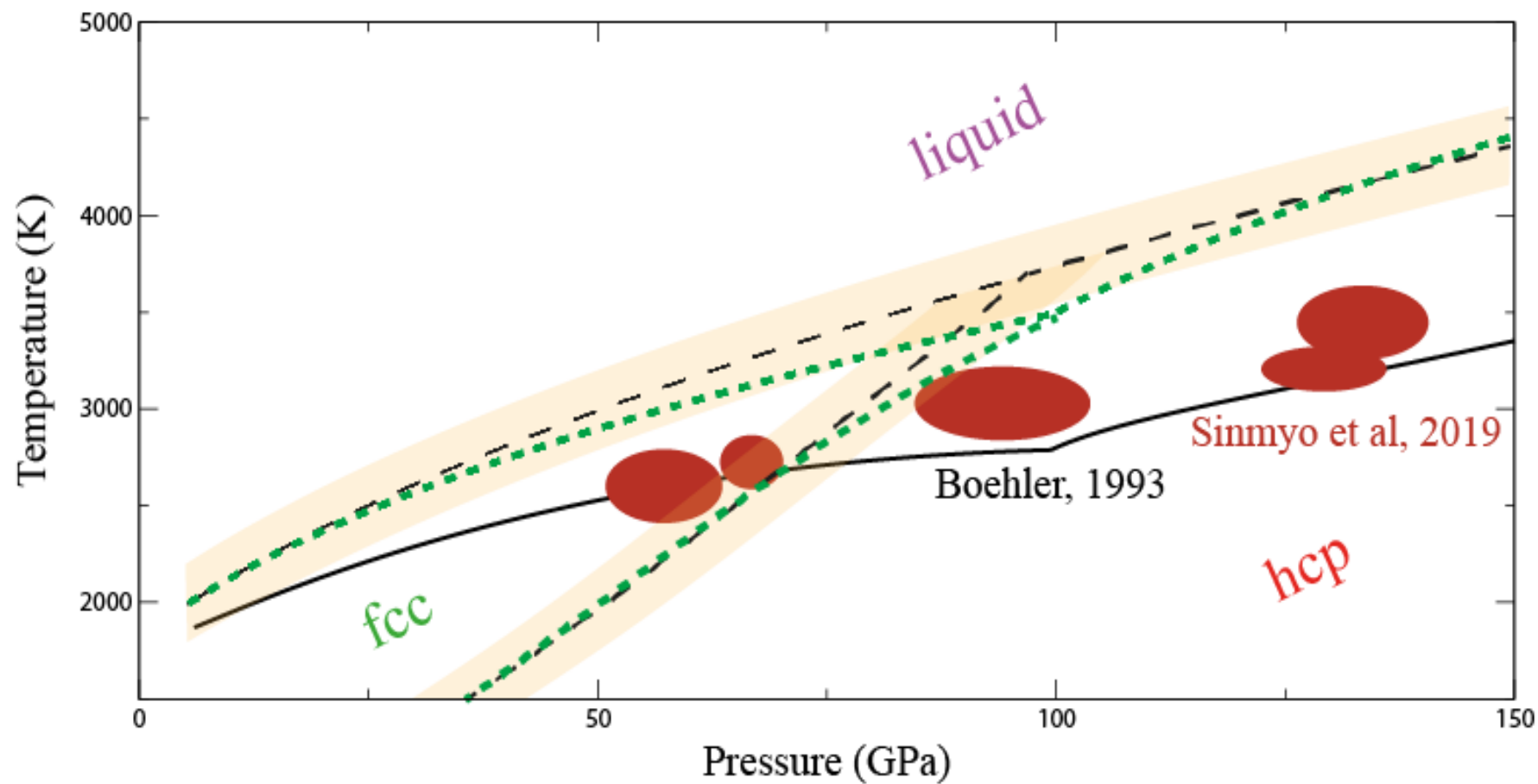
Guillaume Morard¹ , Silvia Boccato² , Angelika D. Rosa², Simone Anzellini³ ,
Francesca Miozzi¹ , Laura Henry², Gaston Garbarino², Mohamed Mezouar², Marion Harmand¹,
François Guyot¹ , Eglantine Boulard¹, Innokenty Kantor^{2,4} , Tetsuo Irifune⁵, and
Raffaella Torchio² 

2018

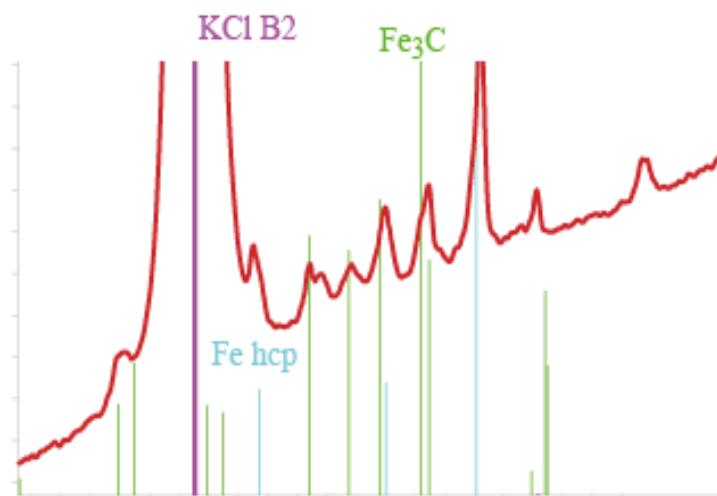


Excellent
 agreement between
 XRD and XAS
 melting
 measurements

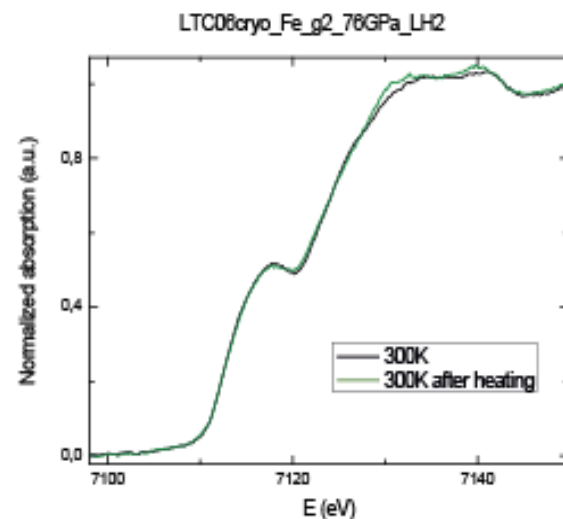
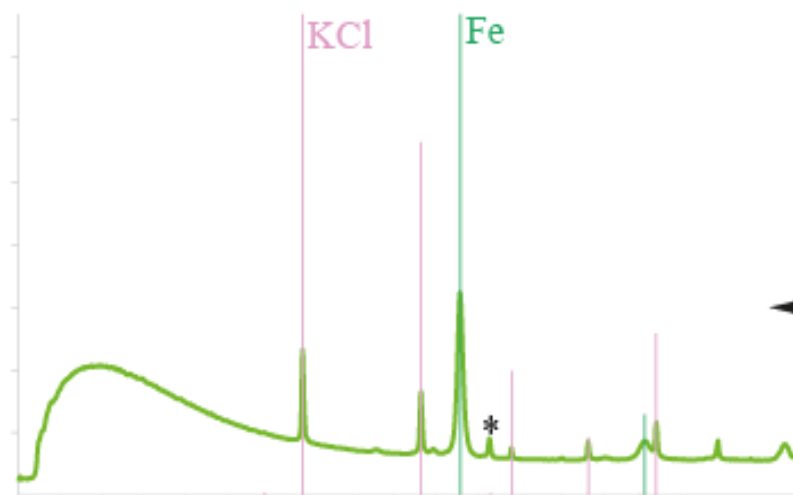
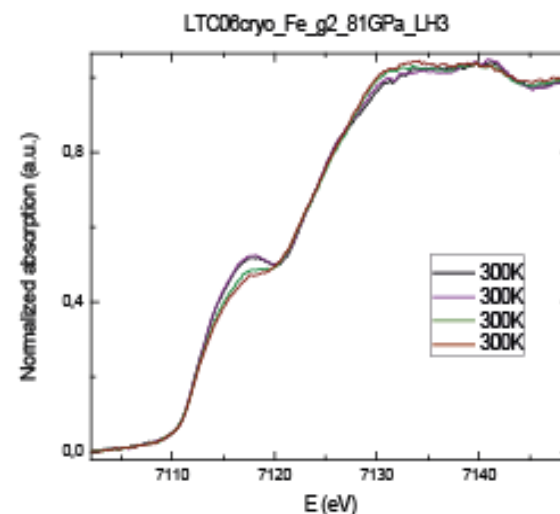
Comparison with previous studies



Diffraction on recovered samples

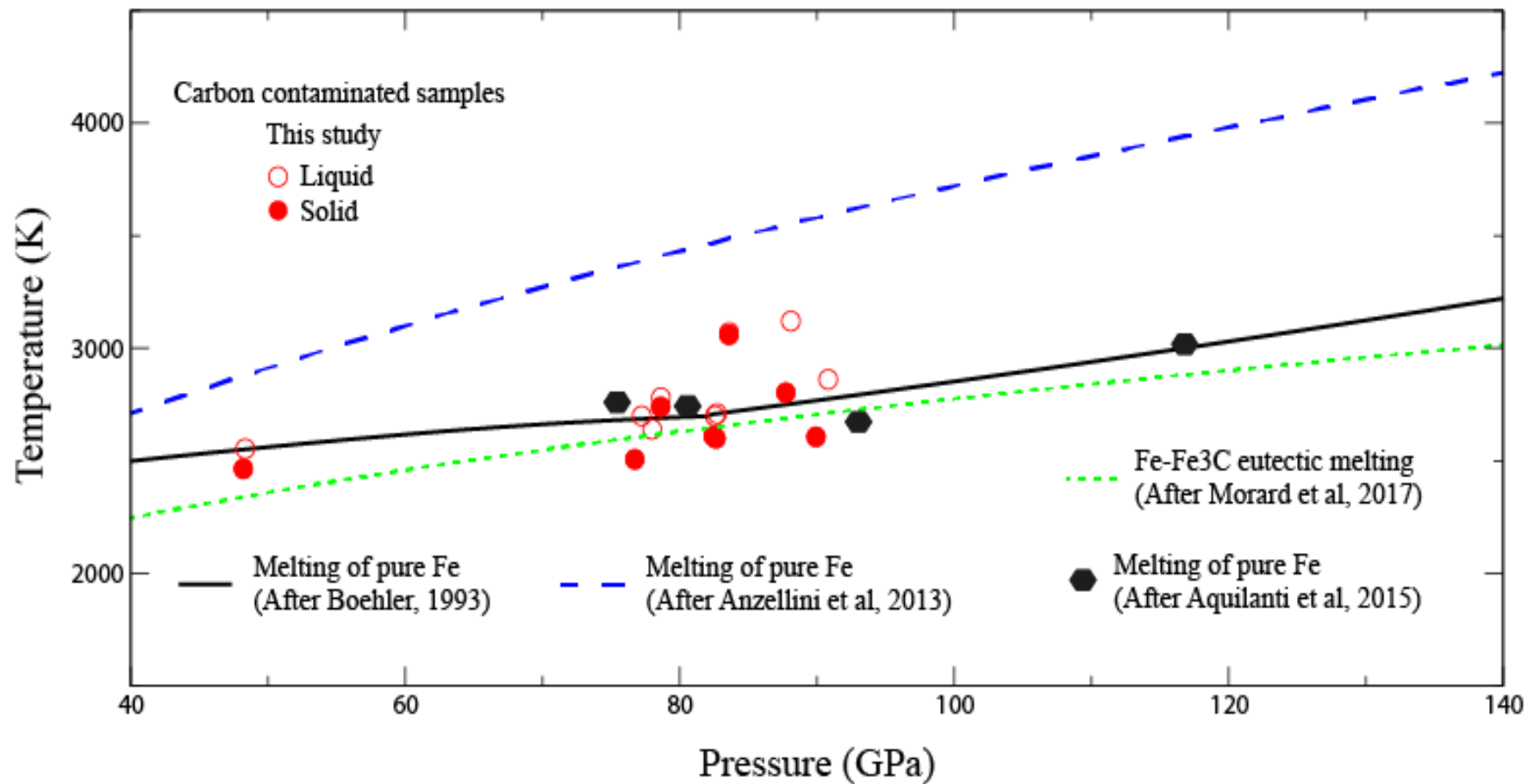


XANES spectra on quench sample between each temperature step

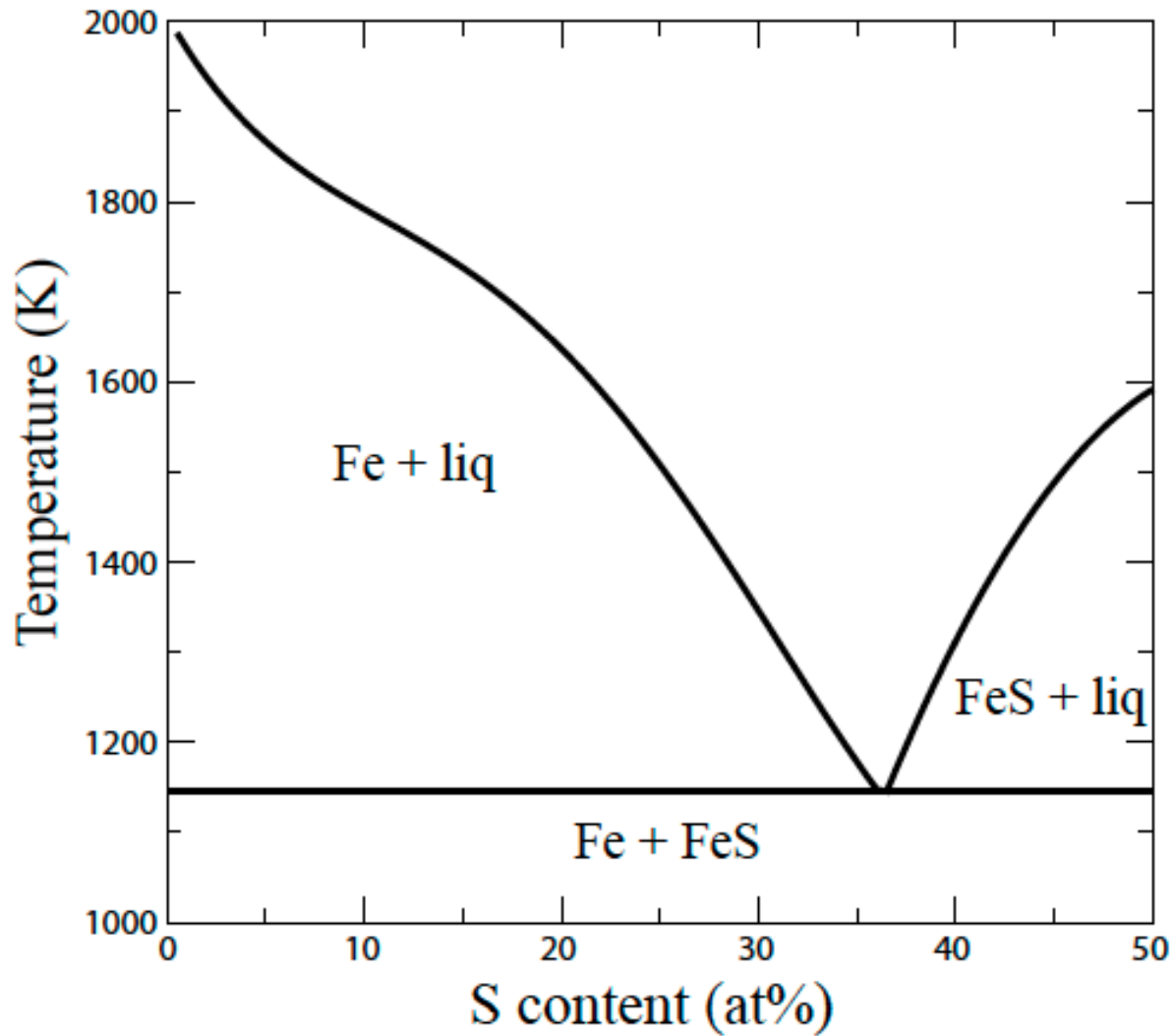


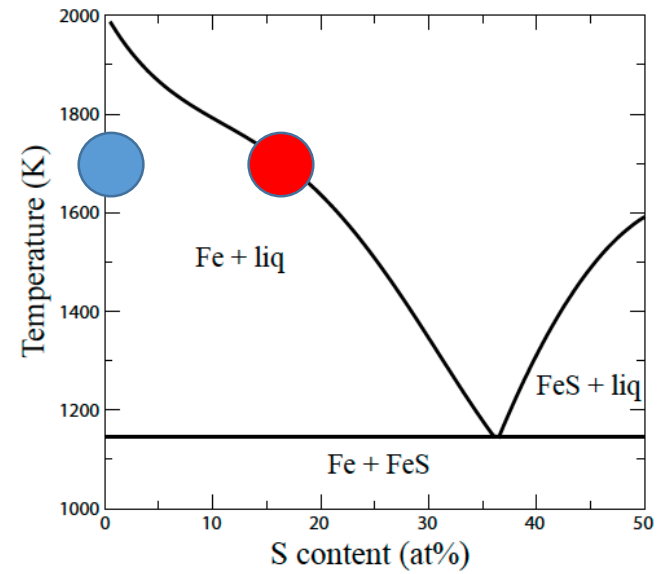
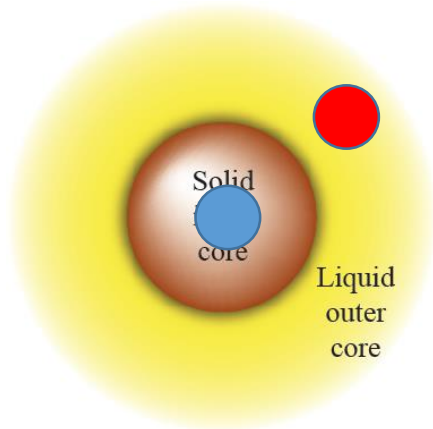
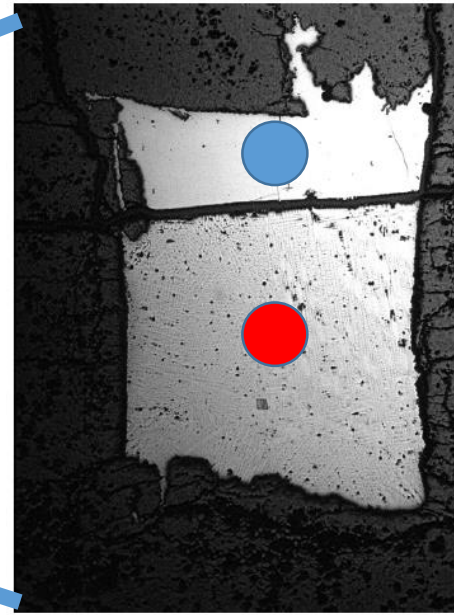
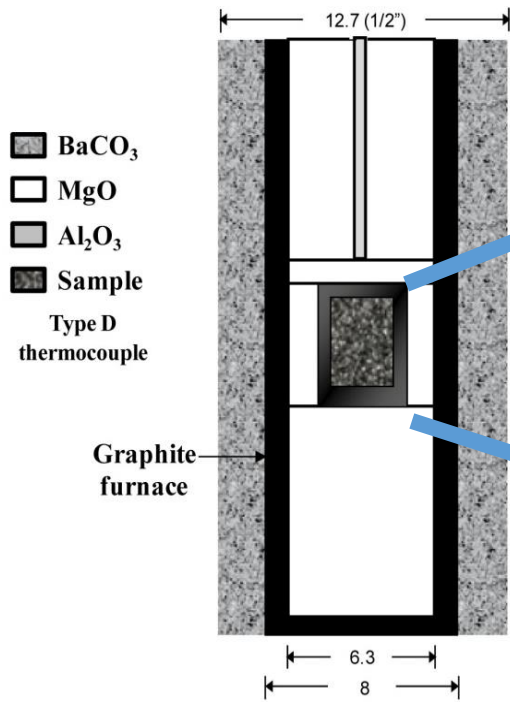
Reactions forming carbides could be clearly identified

Melting of carbon contaminated iron samples

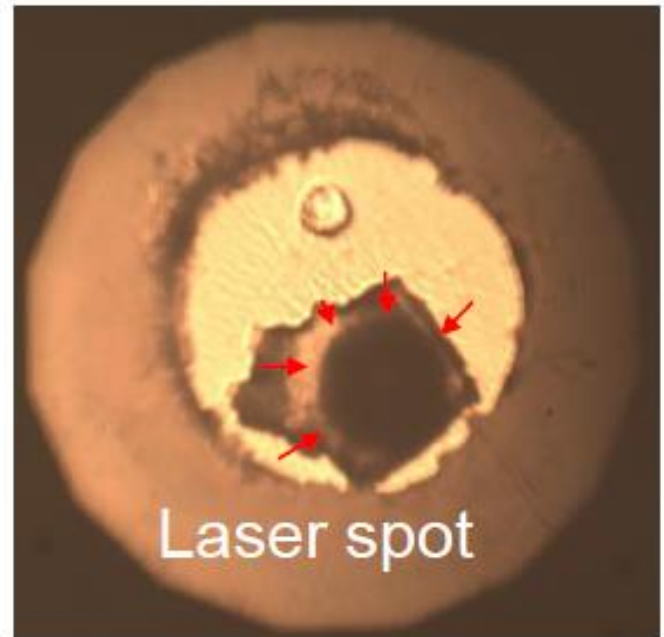
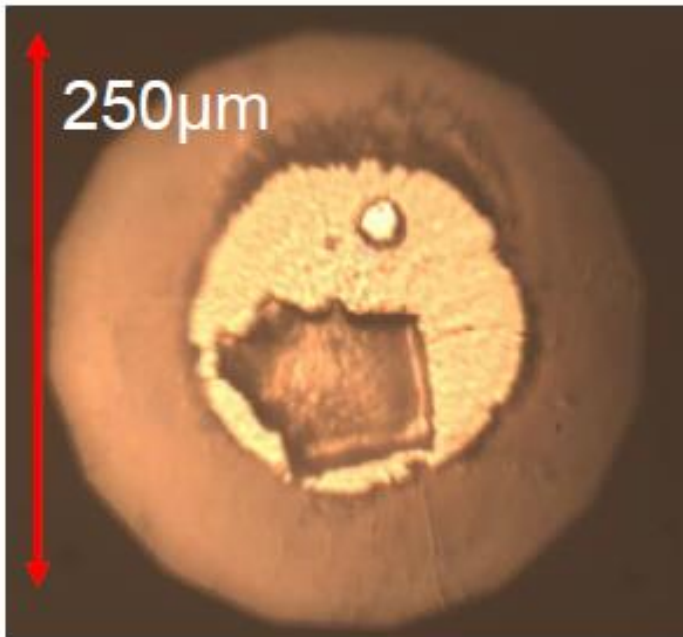


Incongruent melting

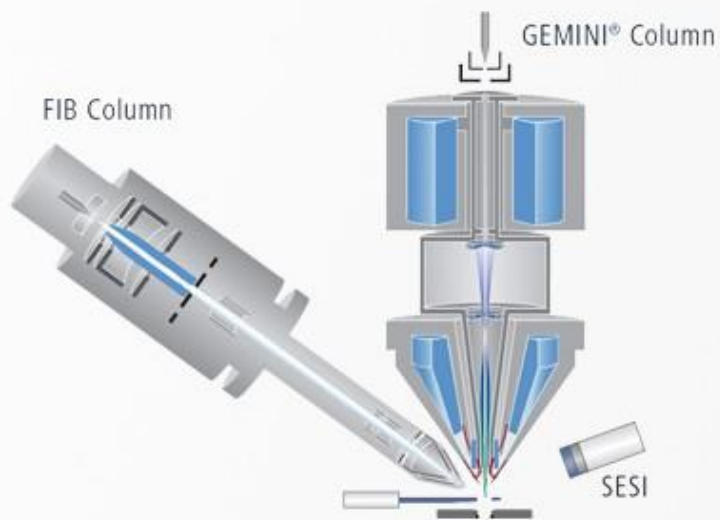




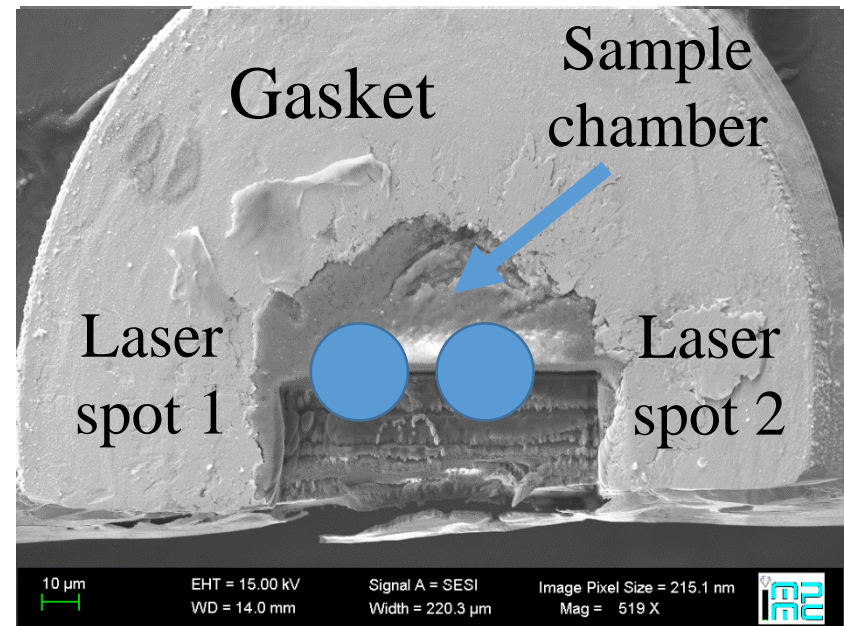
after Buono & Walker, GCA 2011



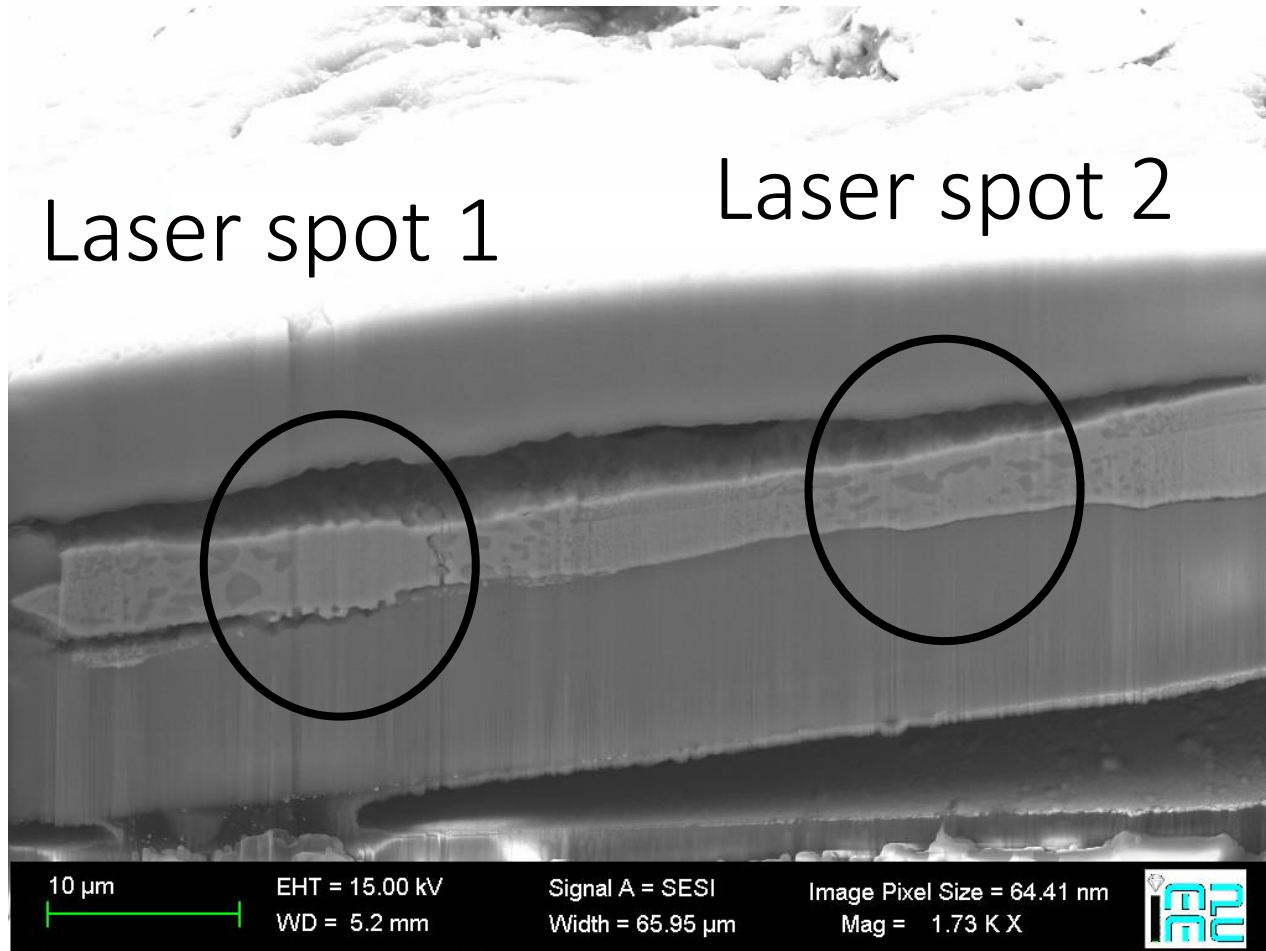
Analysis of post-experiment samples

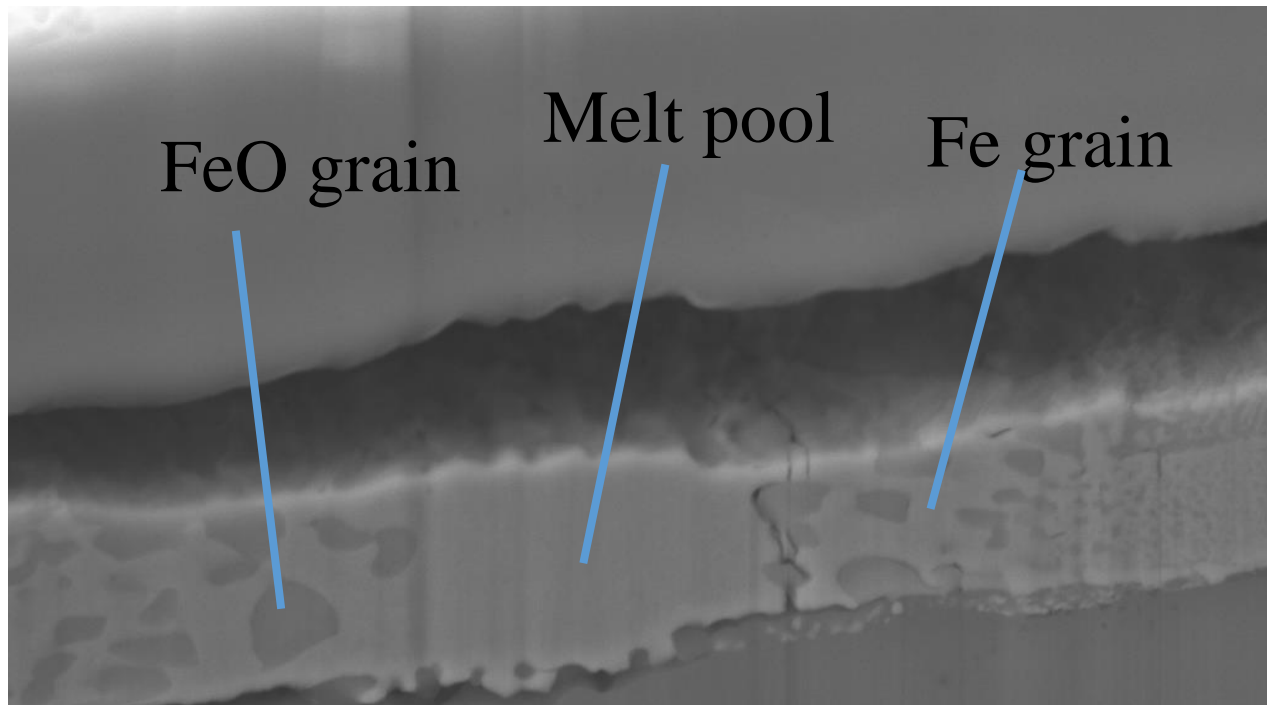


Sample recovered after laser heating experiment at 41 GPa



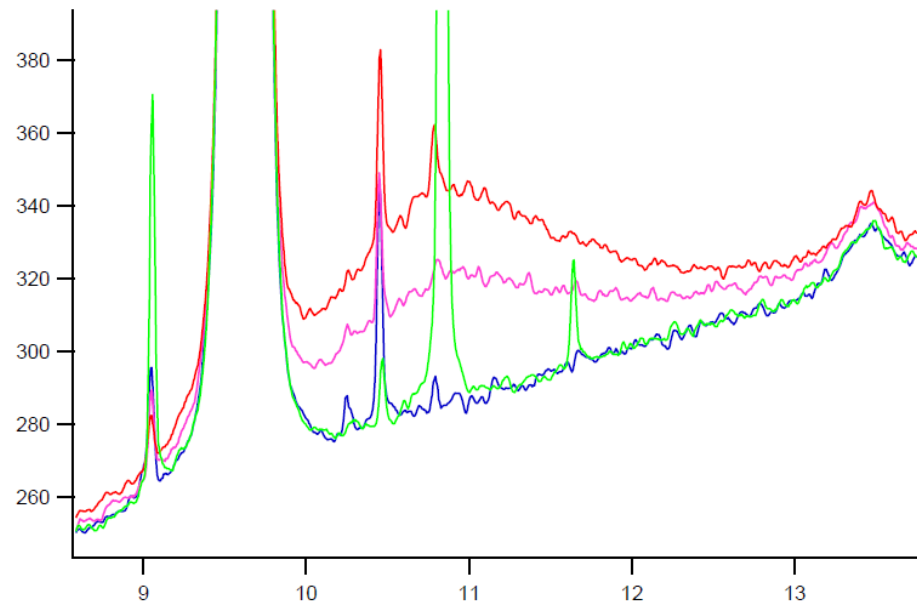
Confirmation from analysis of sample texture after laser heating





2 μ m EHT = 15.00 kV Signal A = SE
WD = 5.2 mm Width = 26.42

- 2110 K
- 2310 K
- 2390 K
- 2550 K

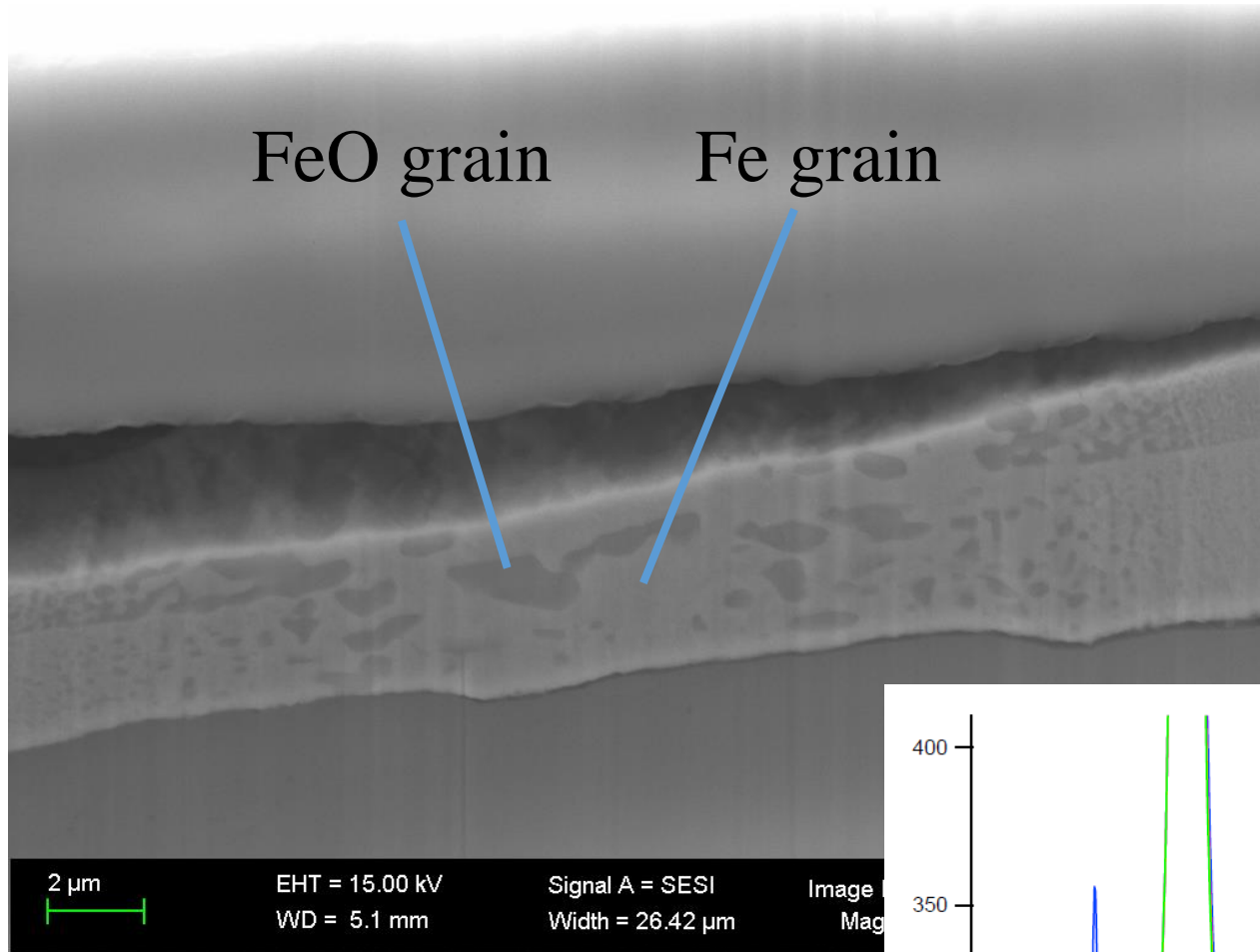


FeO grain

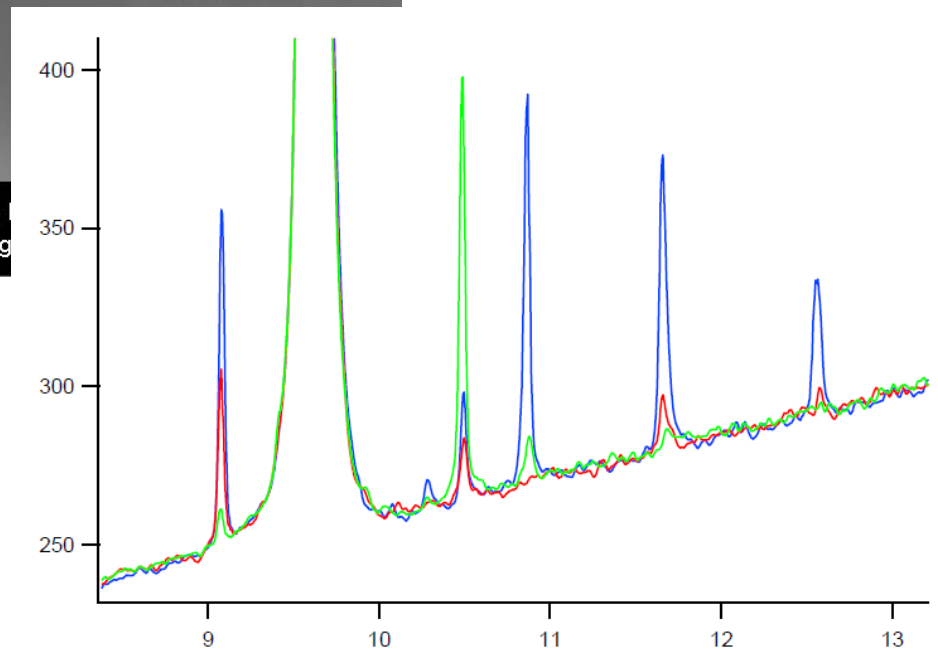
Fe grain

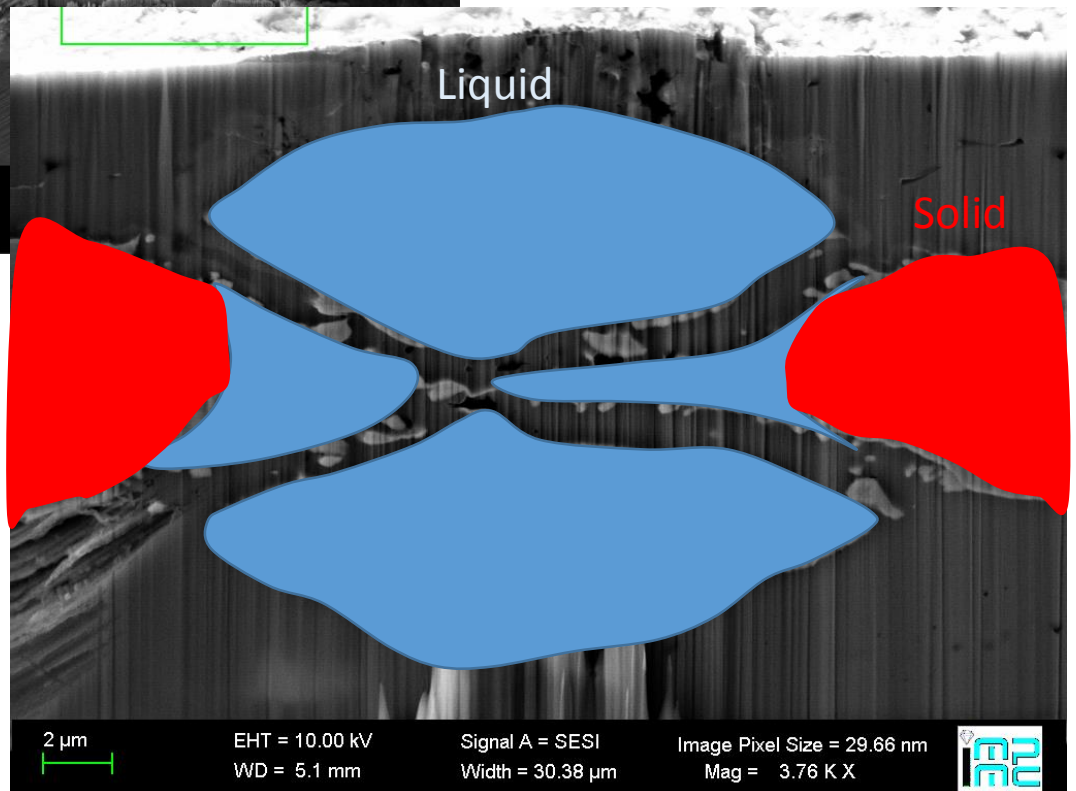
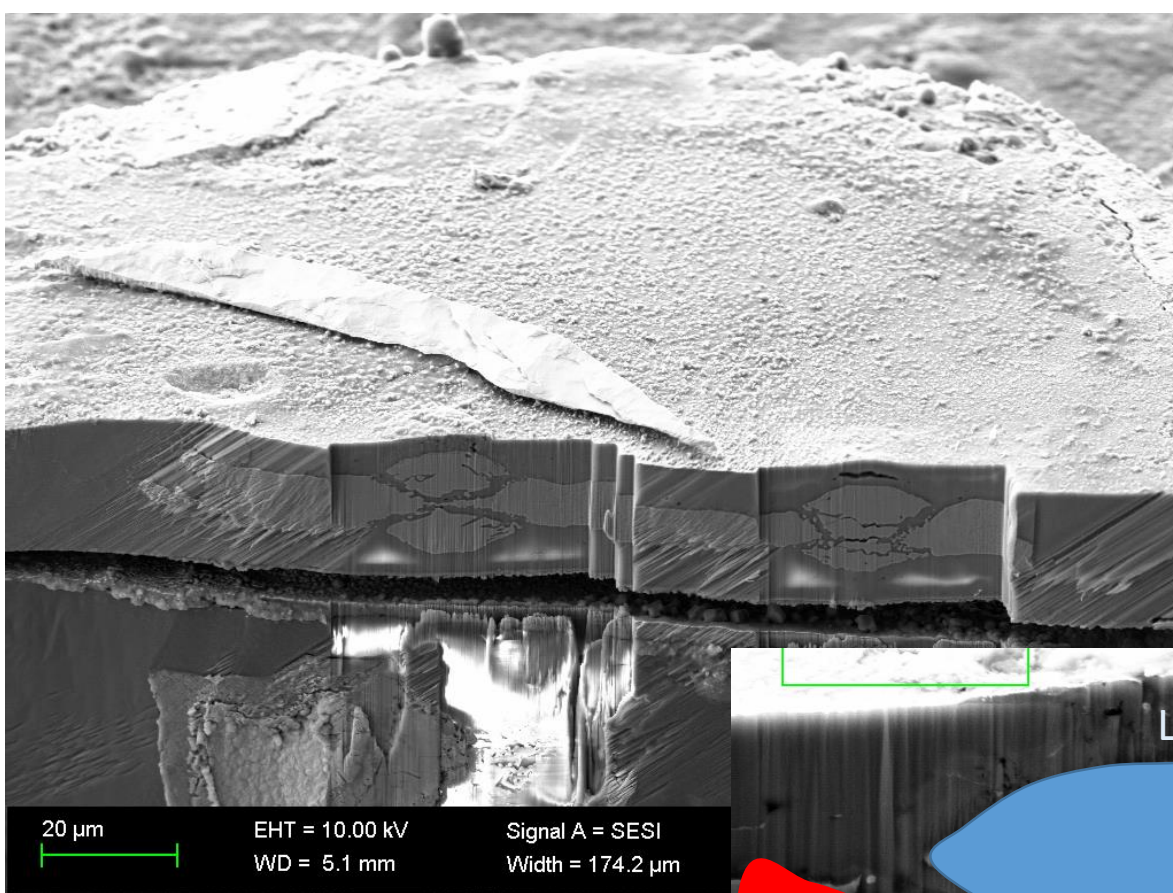
Laser spot 2

Below
melting
temperature

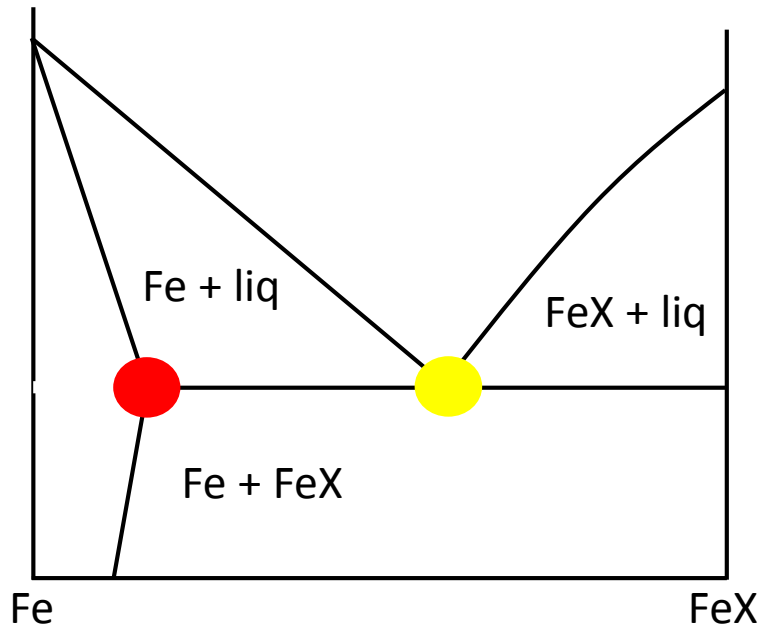


— 2070 K
— 2150 K
— 2170 K

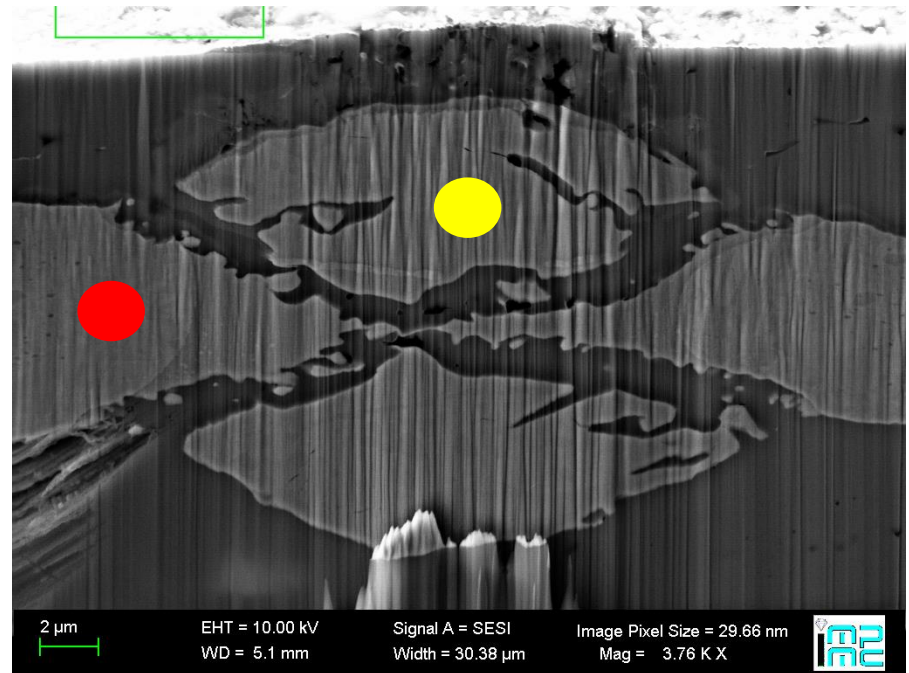


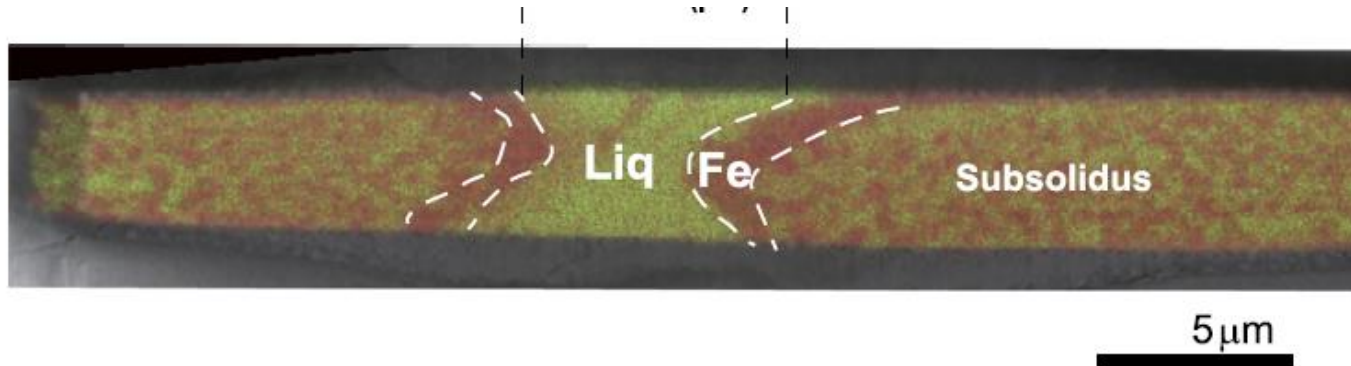


Creating a
planetary core
experimentally

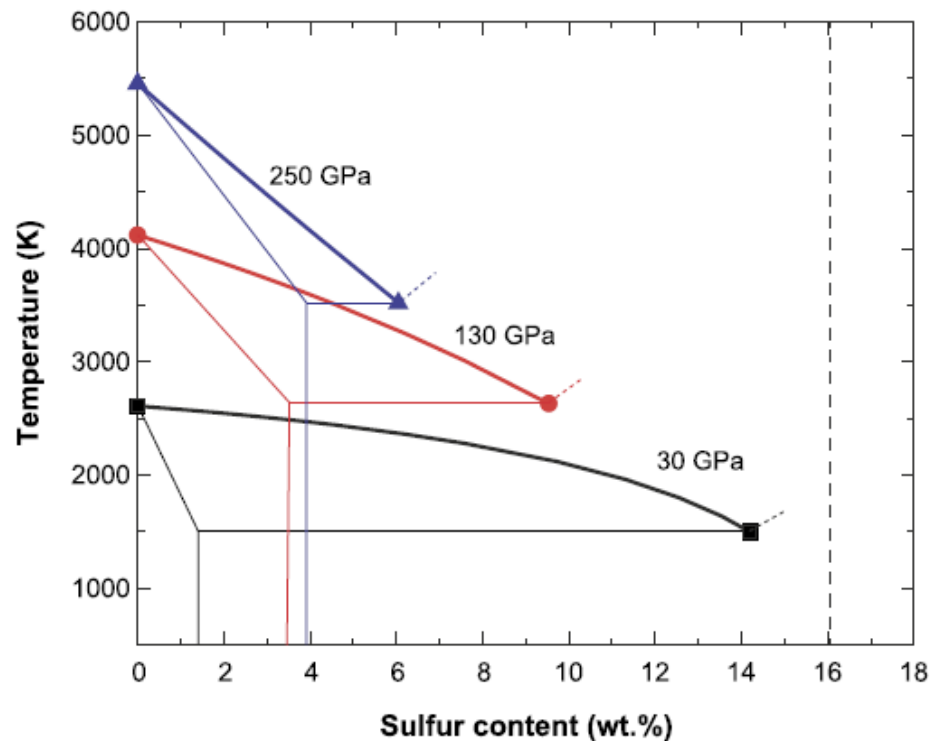


Determination of the
phase diagram under
high pressure



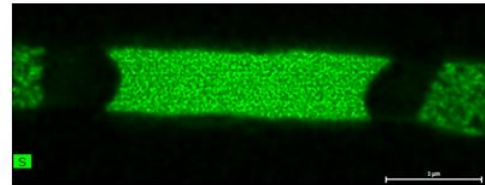
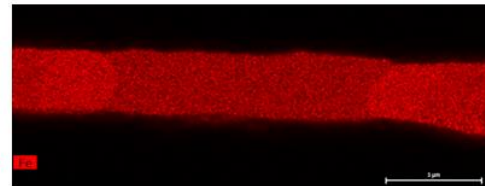
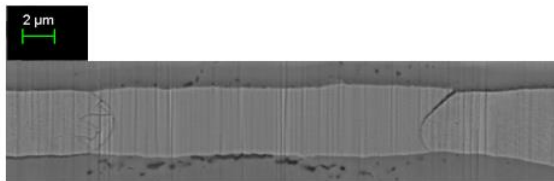


Reconstructing
phase diagrams of
iron alloys under
Earth's core
conditions

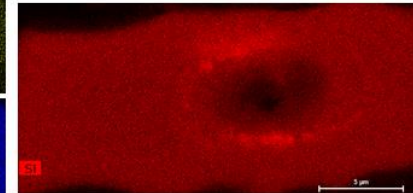
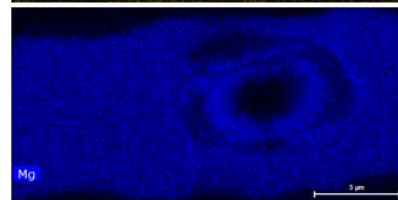
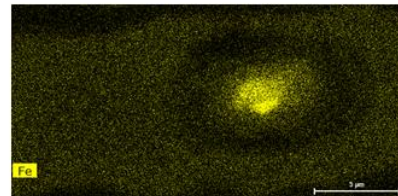
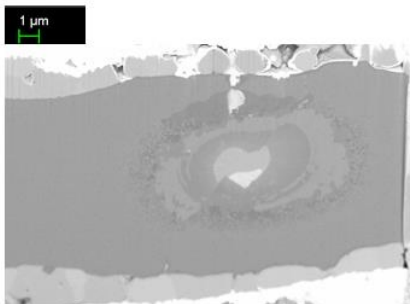


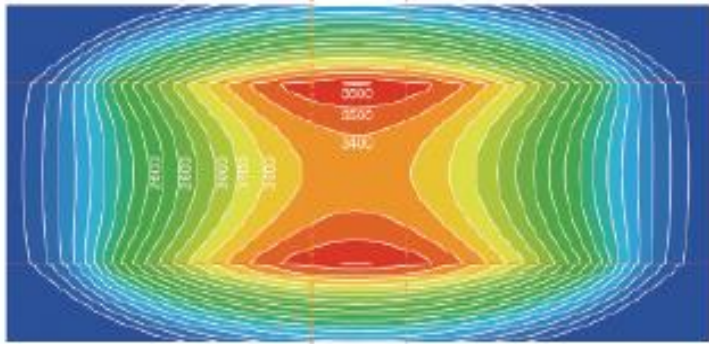
Problem of chemical segregation

Fe-S alloy after melting at 30 GPa



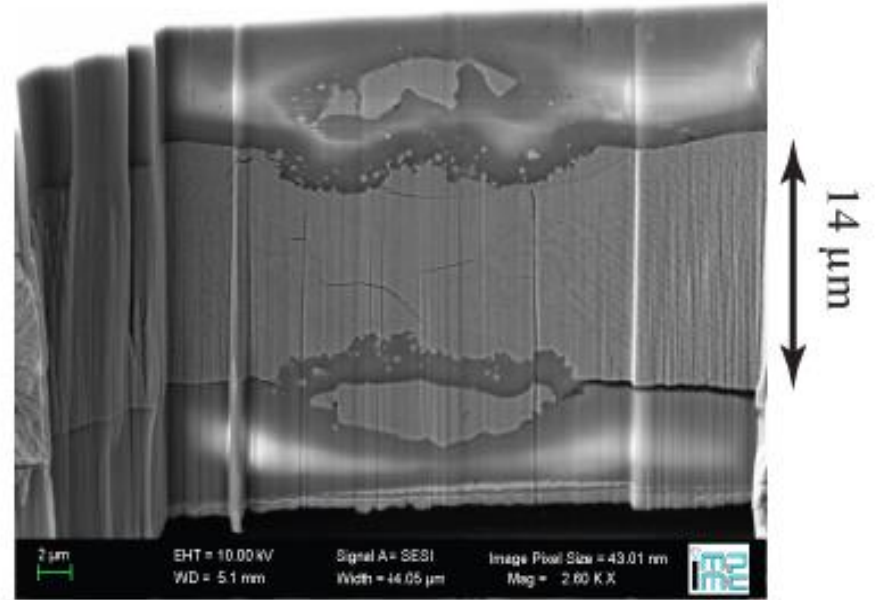
MORB silicate after melting at 65 GPa

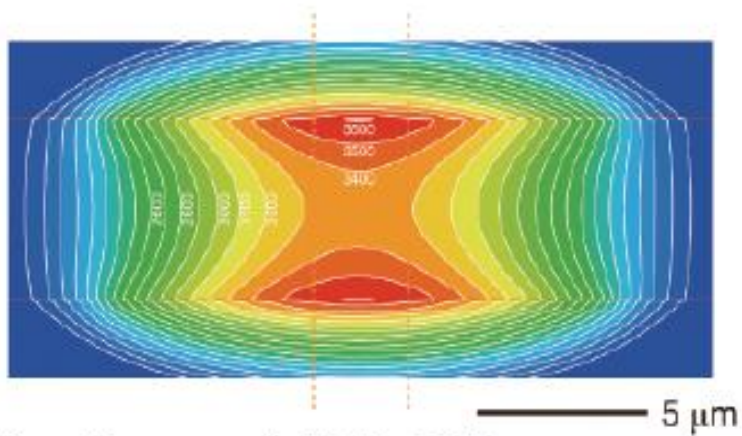




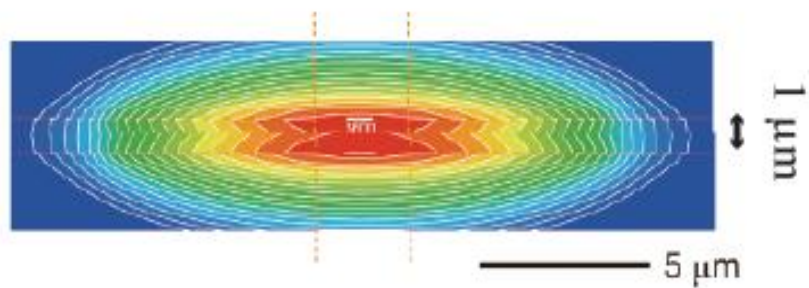
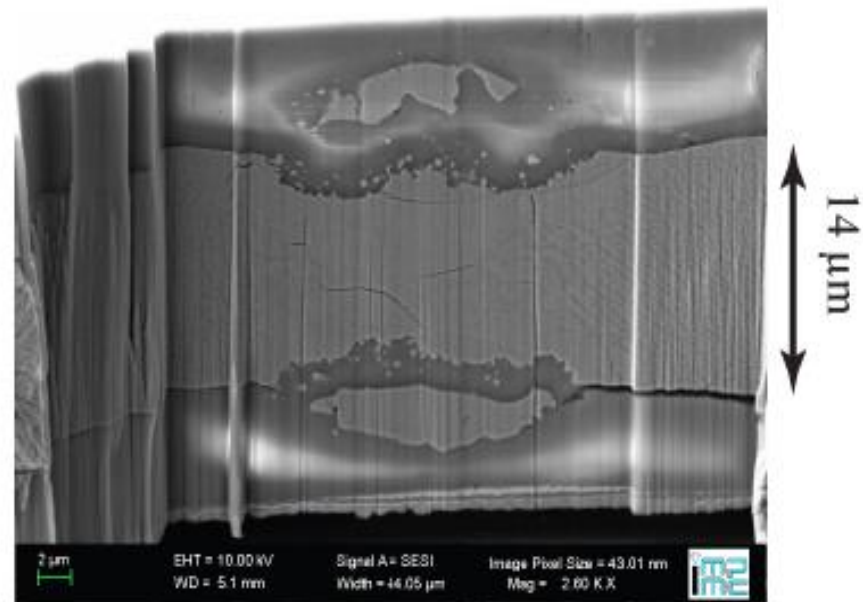
5 μm

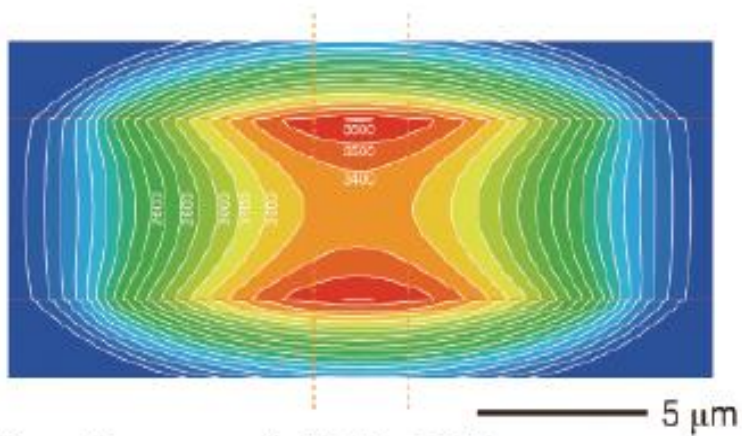
After Sinmyo et al, EPSL, 2019



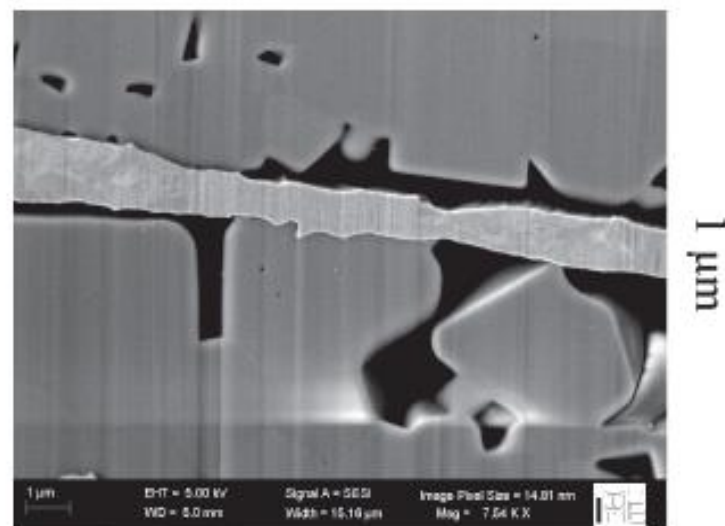
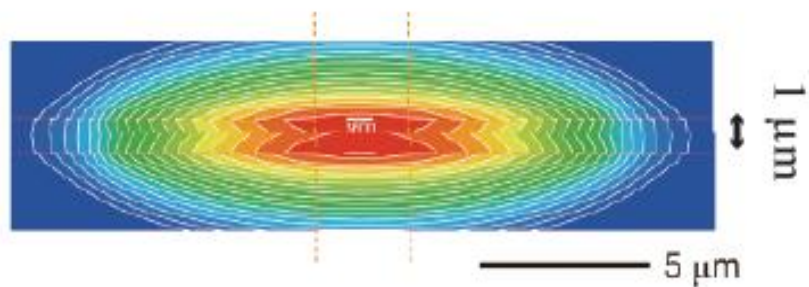
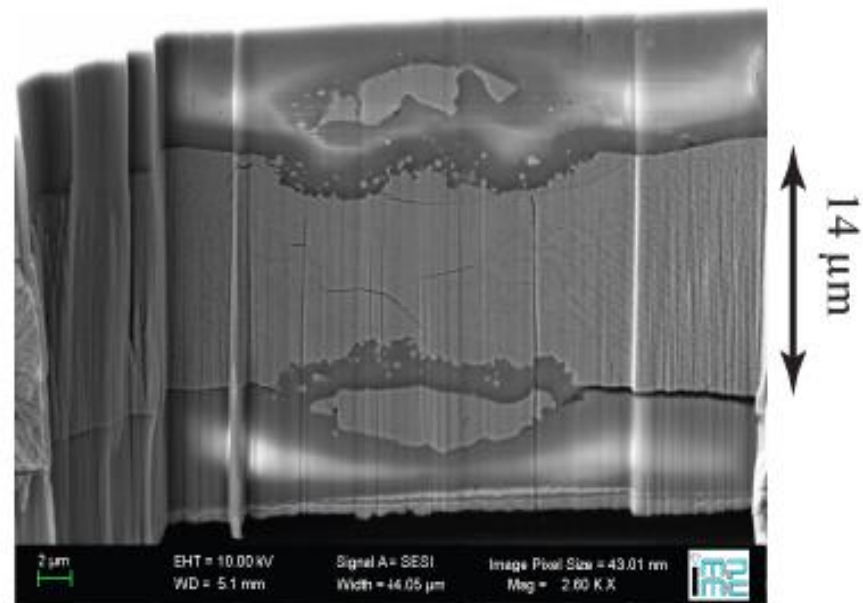


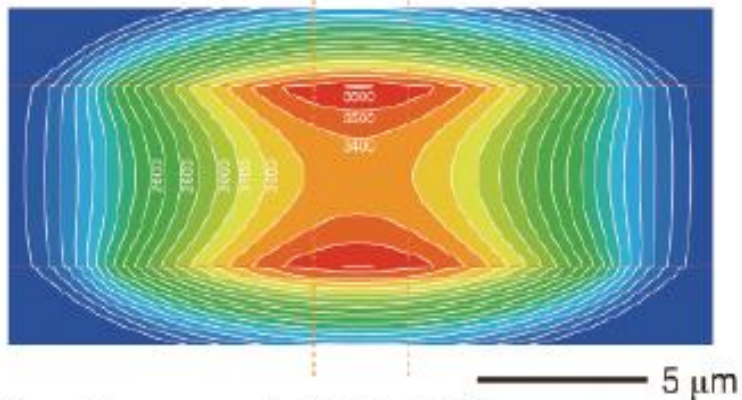
After Sinmyo et al, EPSL, 2019



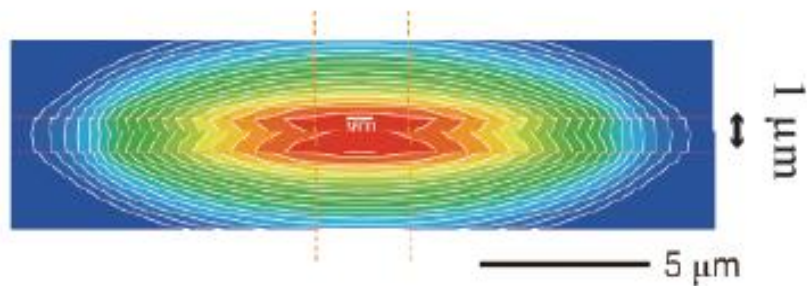
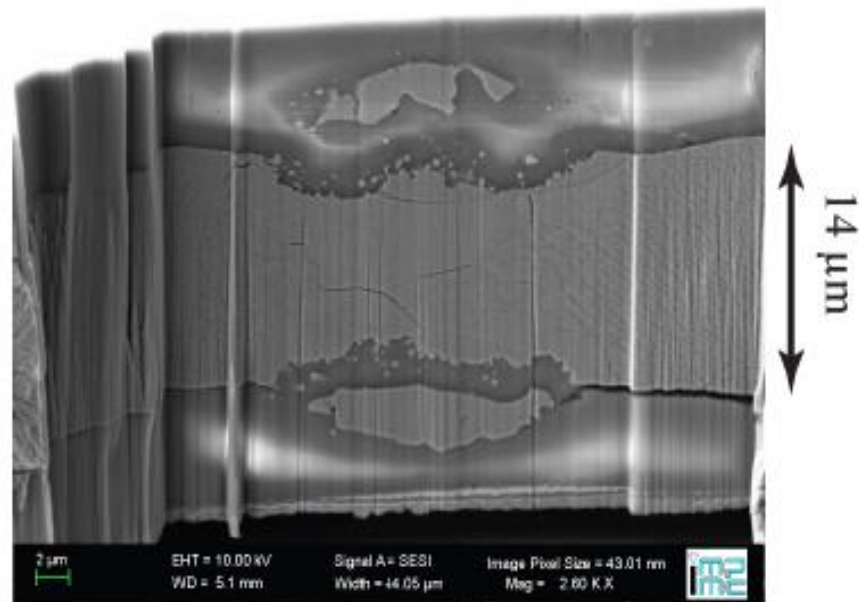


After Sinmyo et al, EPSL, 2019

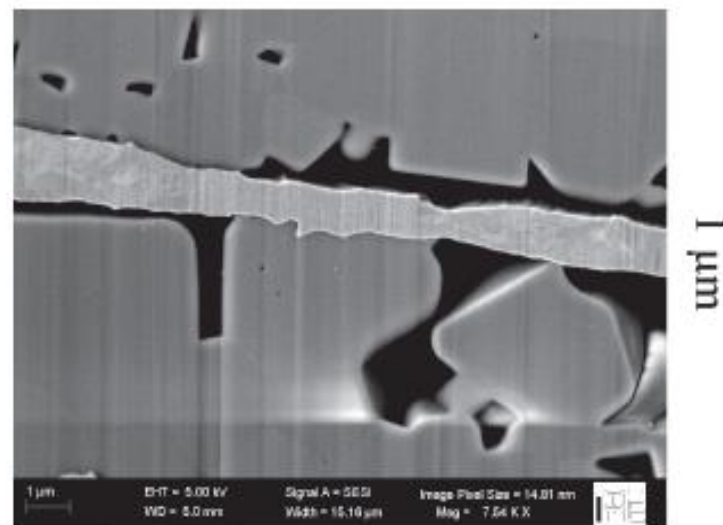




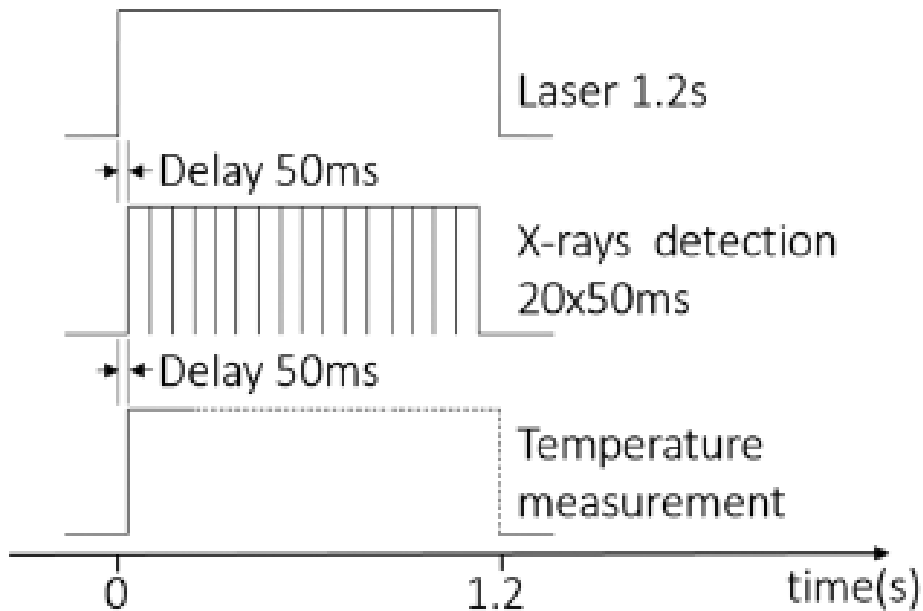
After Sinmyo et al, EPSL, 2019



Temperature gradients minimal in laser heating experiments if sample under high pressure is thinner than $\sim 2\mu\text{m}$



Fast acquisition could be the key

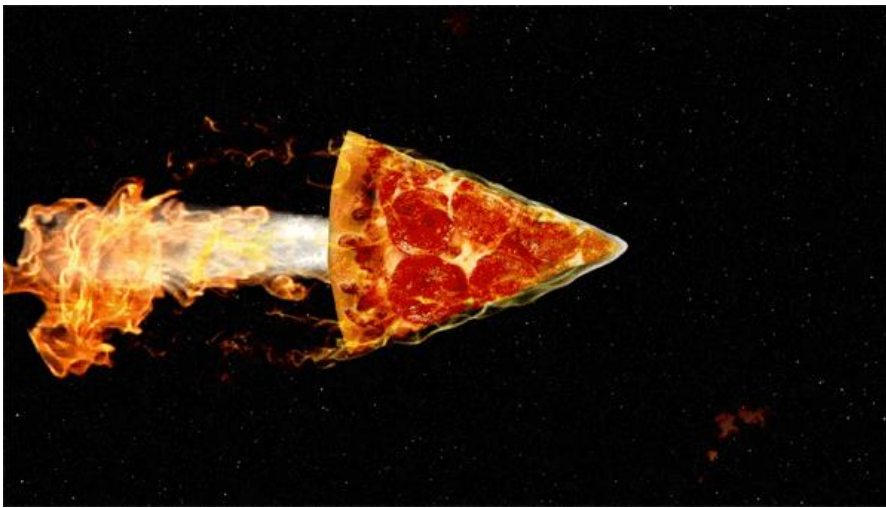


After Boccato et al, JGR, 2017

With the EBS,
flux * 100

Therefore
acquisition time
/100
(CdTe detector
250 Hz)

Data treatment of large amount of data ??



Thank you
for your
attention